RIGA TECHNICAL UNIVERSITY

Andrejs Šiškins

RESEARCH AND DEVELOPMENT OF MULTIFUNCTIONAL POROUS MATERIALS ON THE BASIS OF CLAY AND GLASS WASTE

Summary of the Doctoral Thesis

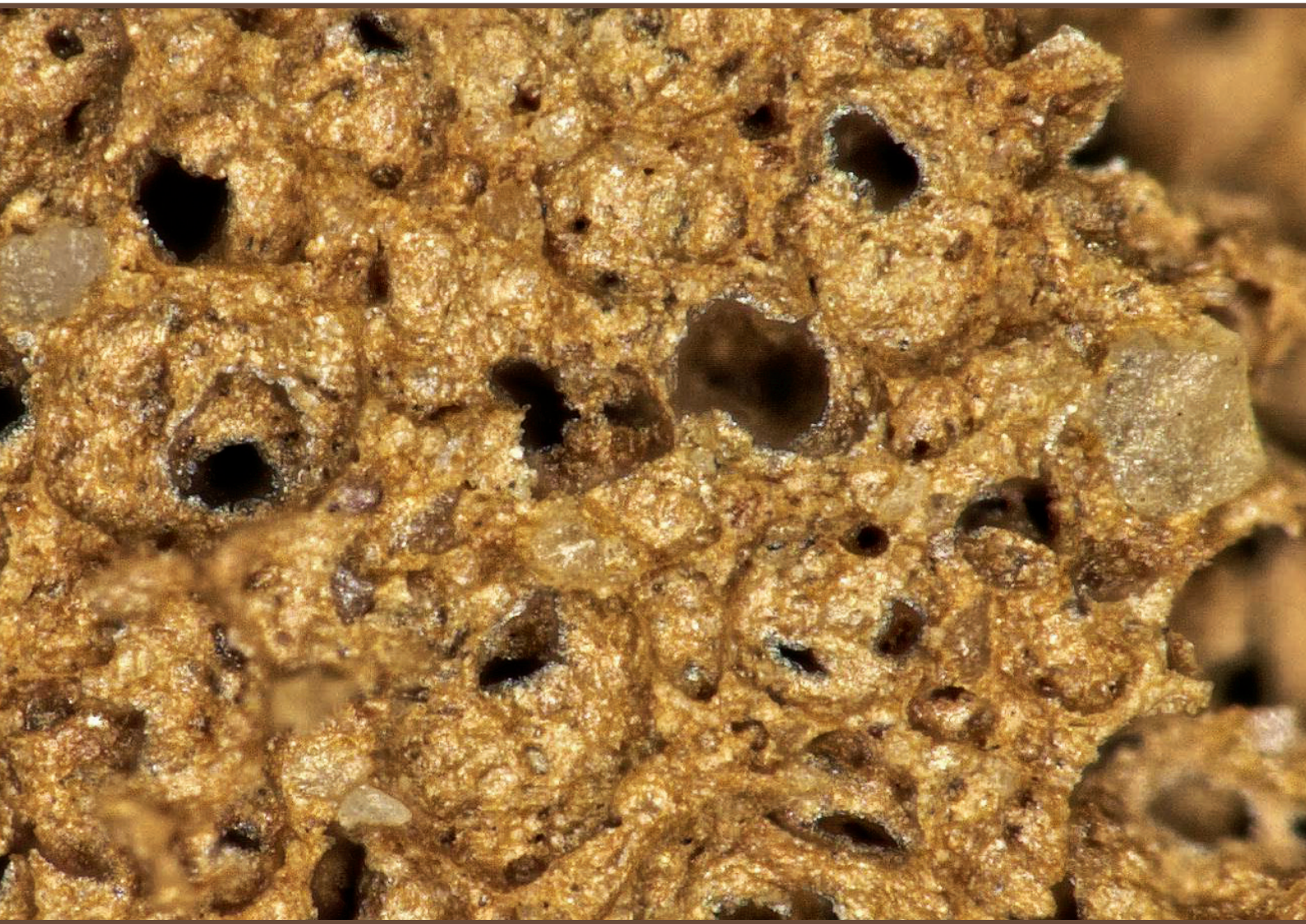

RTU Press
Riga 2021

RIGA TECHNICAL UNIVERSITY
Faculty of Materials Science and Applied Chemistry
Institute of General Chemical Engineering

Andrejs Šiškins
Student of Doctoral Study Programme "Chemical Technology"

RESEARCH AND DEVELOPMENT OF MULTIFUNCTIONAL POROUS MATERIALS ON THE BASIS OF CLAY AND GLASS WASTE

Summary of the Doctoral Thesis

Scientific Supervisors:

Professor Dr. sc. ing.
JURIJS OZOLINS

Professor Dr. habil. sc. ing.
VIKTORS MIRONOVS

RTU Press
Riga 2021

Šiškins, A. Research and Development of Multifunctional Porous Materials on the Basis of Clay and Glass Waste. Summary of the Doctoral Thesis. Riga: RTU press, 2021. 41 p.

Published in accordance with the decision of the Promotion Council "RTU P-01" of 19 April 2021, Minutes No.0030-9.1/21.

https://doi.org/10.7250/9789934226342
ISBN 978-9934-22-634-2 (pdf)

DOCTORAL THESIS PROPOSED TO RIGA TECHNICAL UNIVERSITY FOR THE PROMOTION TO THE SCIENTIFIC DEGREE OF DOCTOR OF SCIENCE

To be granted the scientific degree of Doctor of Science (Ph. D.), the present Doctoral Thesis has been submitted for the defence at the open meeting of RTU Promotion Council on 29 June 2021 at 14:00 online https://rtucloud1.zoom.us/j/9352086644.

OFFICIAL REVIEWERS:

Lead Researcher Dr. habil. sc. ing. Visvaldis Švinka
Riga Technical University, Latvia

Professor Dr. Danutė Vaičiukynienė
Kaunas University of Technology, Lithuania

Professor Dr. ing. Paolo Colombo
The University of Padova, Italy

DECLARATION OF ACADEMIC INTEGRITY

I hereby declare that the Doctoral Thesis submitted for the review to Riga Technical University for the promotion to the scientific degree of Doctor of Science (Ph. D.) is my own. I confirm that this Doctoral Thesis had not been submitted to any other university for the promotion to a scientific degree.

Andrejs Šiškins ……. (signature)

Date: ……

The Doctoral Thesis has been written in Latvian. It consists of an Introduction; 3 Chapters; Conclusions; 79 figures; 23 tables; 26 equations; the total number of pages is 126. The Bibliography contains 216 titles.

ACKNOWLEDGMENTS

I express sincere gratitude to my scientific supervisors – lead researcher Dr. habil. sc. ing. Viktors Mironovs and Professor Dr. sc. ing. Jurijs Ozolinsh – for their everlasting support, help, and patience.

My deepest gratitude goes to Professor Dr. habil. sc. ing. Gundars Mežinskis and to Gaida Sedmale (RTU Silicate Materials Institute) for providing me with basic knowledge in ceramic technologies during my master's studies and inspiring me to continue research in the field of clay ceramic technologies.

I am thankful to all my colleagues from the Rudolfs Cimdins Riga Biomaterials Innovations and Development Centre of RTU, Institute of General Chemical Engineering, Faculty of Materials Science and Applied Chemistry, and, especially, to researcher Dr. Kristaps Rubenis and scientific assistant M. sc. Valentina Stepanova, who supported me through experiments and testing. I would also like to express gratitude to Dr. Janis Baronins and Dr. Mara plotniece who supported me while writing this Thesis.

Thanks to Dr. sc. ing. Aleksandrs Korjakins, Dr. sc. ing. Diana Bajare, and sc. ing. Girts Bumanis (RTU Institute of Materials and Structures Department of Building Materials and Products) for their cooperation and assistance in production and testing of the building blocks.

I thank Dr. Gaurav Goel from the UK, Dr. Igor Štubņa and Dr. Stefan Csaki from Slovakia, and Dr. Aguedal Hakim from Algeria for providing external supervision to my PhD, which resulted in several joint publications that have helped to inform this Thesis.

Last, but not least, my eternal and deepest gratitude goes to my family for their love, patience, and unconditional support.

TABLE OF CONTENTS

LIST OF ABBREVIATIONS

BET – Brunauer–Emmett–Teller method, nitrogen adsorption porosimetry
BTB – dye *Bezaktiv turqouise blue "V-G"*
CCF – clay ceramic foam
CHA – ceramic hollow aggregates
CHA-B – ceramic hollow aggregates containing concrete block
D_{50} – particle size distribution with the value of particle diameter at 50 % in the cumulative distribution
DTA – differential thermal analysis
E_{sp} – specific electricity consumption
EPS – expanded polystyrene
FCA – foamed clay aggregates
FCA-P – foamed clay aggregates with peat coating
FCA-C – foamed clay aggregates with clay coating
KER-B – expanded clay concrete block
MS – model soil
n – degree of crushing
pH_{pzc} – point of zero charge
R^2 – determination coefficient
SEM – scanning electron microscope
TD – thermal dilatometry
UV-VIS – ultraviolet-visible spectroscopy
XRD – X-ray diffraction

GENERAL DESCRIPTION OF THESIS

Topicality of Research

Mineral resources as well as forests, inland and underground water, farmland, etc., are Latvia's national treasures. In Latvia, widespread minerals such as peat, dolomite, and clay are very promising for innovative use [1]. Clay is most widely used for obtaining a wide variety of ceramic materials and products with various structural applications (load-bearing structures, roofing, fire-retardant, and heat-insulating materials, etc.). Depending on the technology, these ceramic materials can have relatively dense and porous structures.

Despite the fact that clays historically have been extensively studied, research regarding their applications for innovative, high value-added products is still ongoing. Unique properties of clay-derived products, like chemical stability, high porosity, high refraction low mass, and thermal conductivity, as well as low specific heat, make them versatile and robust materials.

Rapid technological developments have led to an increase in the volume of industrial and municipal waste, some of which is reusable. One component of municipal solid waste that has a negative impact on the environment is glass containers and fragments, the collection and recycling of which is neglected in Latvia. Over the last decade, developed European countries have recycled more than 80 % of collected glass waste: Germany >83 %, Norway >91 %, Belgium and Sweden >94 %, and Switzerland >96 % [2]. This proactive approach addresses environmental, social, and energy-saving issues, simultaneously. Replacing 10 % of raw clay materials with recyclable glass reduces the energy consumption of glass and ceramic products by 2–3 %. Additional economic efficiency is expected by reducing the environmental damage caused by pollution. Sorted glasses are mainly used for recycling glass containers, production of building materials, foam-glass insulation, and filtering materials, etc. One promising direction for the use of glass waste could be utilization in clay ceramic products.

Therefore, the effect of glass additives on clay ceramic properties was investigated in this Thesis, with the aim to create new, multifunctional porous clay ceramic materials requiring lower energy consumption.

Thesis Objectives and Tasks

The aim of this Thesis was to develop porous, ceramic materials, utilizing Latvian clay and household glass waster, and their processing technology, studying properties of the obtained ceramic materials as well as their practical applications. The following tasks were assigned to reach these objectives:

1) summarize and analyse literature data on Latvian clays, methods of obtaining porous ceramics, and their applications, including sorption processes;
2) evaluate the influence of glass additives and heat treatment temperatures on properties of clay ceramics;
3) develop a method for obtaining ceramic hollow granules and describe their properties and applications;

4) develop a method for obtaining highly-porous clay-glass ceramic foam in form of block and granules and describe their properties and applications;
5) study the adsorption properties of clay-glass ceramic foam in relation to textile dyes with the aim to use them as sorbents in wastewater treatment;
6) develop a possible technological scheme for industrial production of clay ceramic hollow granules, clay foam ceramic granules, and clay foam ceramics.

Scientific Significance and Novelty

The effect of crushed bottle glass additive (5–15 wt. %) on the properties of clay-glass ceramics obtained at relatively low firing temperatures in the range of 700 °C to 1150 °C was systematically studied.

For the first time, technological solutions have been developed for the production of clay-glass ceramic hollow granules using the burnt template method, as well as the production of clay-glass foam ceramics by the direct foaming method.

The adsorption of textile dyes and petroleum products on foam clay-glass ceramics was studied for the first time. Sorption kinetics and sorption isotherms were analysed in this work, and possible sorption mechanisms were evaluated.

Practical Significance

As a result of this research, new methods and recipes for the production of porous clay ceramics at relatively low firing temperatures, containing recycled solid municipal waste, e.g., glass fragments, have been proposed. The possibility of obtaining porous clay-glass ceramics in the form of hollow pellets has been demonstrated using a cylindrical granulation machine and burn-out template method, as well as direct foaming in a rotary mixer-disperser with a cavitation effect. Ceramic hollow granules (Patent No. LV 14822 B of the Republic of Latvia) were obtained for the production of lightweight building blocks with increased mechanical strength. Clay-glass foam ceramics, in the form of granules or blocks, can be used as sorbents for textile dyes and petroleum products, and these ceramic building blocks are proposed for improved thermal insulation properties of *Keraterm*^{TM} (Latvian Patent No. LV 15188 B).

Thesis for Defence

Solid household waste-glass cullet can be used to obtain clay-glass ceramics at lower firing temperatures, providing relatively good technological properties and, thus, addressing environmental and social issues.

Clay-glass foam ceramics can be obtained in the form of hollow granules, using a combination of rotary cylinder granulation and sacrificial template methods, or in the form of foam, by direct foaming in a mixer-disperser with a cavitation effect.

Clay foam ceramics are characterized by an increased sorption capacity of textile dyes and petroleum products.

Approbation of the Research Results

The main results of the Thesis have been published in five peer-reviewed journal publications and nine conferences theses. Two Latvian Republic patents have been awarded, and one patent application has been submitted.

Publications (indexed in *SCOPUS*)

1. **A. Shishkin,** J. Baronins, V. Mironovs, F. Lukáč, I. Štubňa, and J. Ozolins, "Influence of glass additions on illitic clay ceramics," *Materials (Basel).*, vol. 13, no. 3, pp. 1–15, Jan. 2020.
2. T. Húlan, I. Štubňa, **A. Shishkin,** J. Ozolins, Š. Csáki, P. Bačík, and J. Fridrichová, "Development of Young's modulus of natural illitic clay during heating and cooling stage of firing," *Clay Miner.*, vol. 54, no. 2, pp. 1–25, Jul. 2019.
3. **A. Shishkin,** G. Bumanis, K. Irtiseva, J. Ozolins, and A. Korjakins, "Clay ceramic hollow sphere—cement syntactic foam composite for building applications," *Key Eng. Mater.*, vol. 800, pp. 228–234, Apr. 2019.
4. **A. Shishkin,** A. Laksa, V. Shidlovska, Z. Timermane, H. Aguedal, and V. Mironovs, "Illite clay ceramic hollow sphere—obtaining and properties," *Key Eng. Mater.*, vol. 721, pp. 316–321, Dec. 2016.
5. **A. Shishkin**, H. Aguedal, J. Peculevica, D. Newport, G. Goel and J. Ozolins, "Influence of waste glass in the foaming process of open cell porous ceramic as filtration media for industrial wastewater," *J. Clean. Prod.*, vol 282, p. 124546, Feb. 2021.
6. **A. Shishkin**, G. Goel, J. Baronins, J. Ozolins, C. Hoskins, and S. Goel, "Using circular economy principles to recycle materials in guiding the design of a wet scrubber-reactor for indoor air disinfection from coronavirus and other pathogens", *Environ. Technol. Innov.*, vol. 22, p. 101429, May 2021.

Conferences

1. **A. Šiškins**, "Valorization of glass and clay in the production of new multifunctional porous ceramics," in *Materials Science and Applied Chemistry Conference*, 2019, p. 31. Oct. 2019., Riga. Oral report.
2. **A.Šiškins**, J. Peculeviča, H. Aguedal, J. Ozoliņš, and V. Mironovs, "Production and properties of low-temperature glass-ceramic foam based on illie Latvian clay," in *Clays and Ceramics 2018*, 2018, pp. 42–43. Jan. 2018, Riga. Oral report.
3. **A. Shishkin,** A. Laksa, V. Shidlovska, Z. Timermane, H. Aguedal, V. Mironovs, and J. Ozolins, "Illite clay ceramic hollow sphere – obtaining and properties," in *25th International Baltic Conference on Engineering Materials & Tribology*, 2016, p. 37. Nov. 2016, Riga. Oral report.
4. **A. Shishkin**, A Korjakins, and V. Lapkovskis, "Influence of the firing temperature on the illite clay ceramic foam with waste glass powder addition," in *25th International*

Baltic Conference on Engineering Materials & Tribology 2016, p. 40, 2016, Nov. 2016, Riga. Oral report.

5. **A. Shishkin,** V. Mironovs, D. Goljandin, and A. Korjakins, "Influence of milled waste glass to clay ceramic foam properties made by direct foaming route," in *Proceedings of ICEMT 2016: 18th International Conference on Engineering Materials and Technology*, pp. 624–67, Jun. 2016, Riga. Oral report.
6. **A. Shishkin**, A. Laksa, Z. Timermane, V. Šidlovska, V. Mironovsa, and J. Ozoliņš, "Ar kombinēto metodi iegūtu mālu keramikas porainu granulu sorbcijas pētījumi (in Latvian), Sorption study for porous clay ceramic pellets obtained with the combined method," in *International Interdisciplinary Symposium Clays and Ceramics*, p. 44, 2016. Jan. 2016, Riga. Poster.
7. **A. Shishkin**, A. Laksa, Z. Timermane, V. Šidlovska, and J. Ozoliņš, "Mālu dobo keramisko sfēru sorbcijas īpašību pētījumi (in Latvian), Sorption properties of clay ceramic hollow spheres," in *International Interdisciplinary Symposium Clays and Ceramics*, p. 45, 2016. Jan. 2016, Riga. Poster.
8. **A. Shishkin,** A. Korjakins, and V. Mironovs, "Using of cavitational disperser, for porous ceramic and concrete material preparation," *in ICEMT 2015: 17th International Conference on Engineering Materials and Technology*, pp. 734–737, 2015. Jun. 2015, Riga. Oral report.
9. **A. Shishkin,** V. Mironovs, J. Baronins, A. Laksa, and J. Ozolinsh, "Clay ceramic hollow spheres: Method of obtaining, properties, possible application," in *CellMAT 2014*, p. CD, 2014, Dresden. Oral report.

Patents

1. **A. Šiškins,** A. Korjakins, V. Mironovs, J. Ozoliņš. "Eco-friendly porous material for ienhancement of insulation properties of hollow building blocks and a method for obtaining thereof," LV Patent 15188 B, 20.02.2017
2. **A. Šiškins,** V. Mironovs, J. Baroniņš, J. Treijs. "Sorbent with ferromagnetic properties," LV Patent 14822 B, 20.03.2014

1. SUMMARY OF LITERATURE REVIEW

Information about illite clay transformation during thermal sintering, the applicability of wastes in the production of ceramics, and a short description about grinding, agglomeration, and production of porous ceramic is summarized in this literature review. Clay is widely used in the production of a variety of ceramic materials and technical products. While clays have been extensively studied, the growing demands on physical and mechanical properties of these materials, as well as their morphology, have contributed to a rapid increase in the number of research publications on this material.

As living standards of the population increases and technology develops, household and technological waste deposited in landfills is increasing rapidly. Between 1995 and 2015, the amount of municipal waste in Europe increased by 366 % [3], of which 15.7 million tonnes were generated in 2014 by the second most commercially important packaging material, glass [4]. A number of authors [5]–[8] have studied the possibility of utilizing this high-energy material in clay ceramic products. The presence of glass in fired ceramics reduces firing temperature, shrinkage, and water absorption [9]. The development of low density, highly porous ceramic materials is one way to support the European Union's (EU) requirements for reducing energy consumption and CO_2 emissions. The utilization of glass in the production of such materials promotes the use of recycled materials, which is also one of the most important goals in the EU's long-term development plan. European glass production (Table 1.1) is growing all the time. The production of container glass ranks first in terms of share (44.5 %) among all glass products produced in Europe.

Table 1.1

Glass Production by Types in Europe [10], Thousands of Tons

Glass type	Year				
	2014	2015	2016	2017	2018
Container glass	20 146	20 319	21 025	21 537	21 755
Float glass	9284	9641	9835	10 665	10 643
Tableware and Crysal	1050	1080	1181	1253	1337
Glass fibres	658	677	702	700	808
Other glasses	975	1218	1178	1052	861

Table 1.2 shows the average glass compositions reported in the literature for different types of glass waste that were used for the modification of ceramics, including bulk glass and mixed municipal waste glass. As follows from the data in Table 1.2, the average composition of glass waste varies by no more than 1 % and the composition of glass as a secondary raw material can be considered to be sufficiently independent. In case 5 % to 20 % by weight of secondary glass additives are used for the production of clay ceramics, changes in the composition of the glass may cause changes in the composition of the obtained ceramic materials in the range of no more than 0.2 %. Therefore, the use of bulk glass waste is an important raw material resource for obtaining new materials.

Table 1.2

Waste Container Glass Average Chemical Composition

Glass	Chemical Composition									Reference
	SiO_2	Al_2O_3	MgO	CaO	Na_2O	K_2O	SO_3	Other	LOI	
Float glass	71.1	1.40	0.83	10.6	14.2	0.3		Fe_2O_2-0.16	–	[11]
Green container glass	71.2	1.60	1.57	10.8	13.2	0.6	–	Fe_2O_2-0.32 Cr_2O_3-0.2	–	[12]
Transparent container glass	72.1	1.60	1.50	10.9	13.0	0.6	–	–	–	[12]
Brown container glass	72.1	2.19	0.70	10.5	13.7	0.2	–	Fe_2O_2-0.22 Cr_2O_3-0.1	–	[12]
Mixed container glass	70.2	2.10	–	9.5	16.6	–	–	Fe_2O_2-0.1	1.5	[13]

The European Union pays great deal of importance to reduction of energy consumption in Member States. The Energy Efficiency Directive 2012/27/ES [14] has required to reduce energy consumption by 20 % by 2020. Cellular ceramic building blocks are widely applied in construction process in order to improve the energy efficiency of new residential buildings. Such construction blocks characterize by vertically oriented channels. *Keraterm* construction blocks (*AS Lode*, Latvia) are well known in the Baltic region, with a thermal conductivity coefficient (λ) ranging from 0.2 $W \cdot m^{-1} \cdot K^{-1}$ to 0.3 $W \cdot m^{-1} \cdot K^{-1}$ [15]. Nevertheless, the commercially available ceramic blocks do not meet the growing energy efficiency requirements for the construction of near-zero energy buildings. Highly porous ceramic materials can be considered as potentially effective thermal insulation products. The increasing demand for enhanced physical and mechanical properties, as well as morphology led to a rapid increase in the number of research publications in the last decade [16].

Porous ceramic products are one of the most promising sustainable materials for the filtration of drinking water, treatment of wastewater from inorganic substances, and collection of leaked oil products from the aquatic environment. These properties are supported by adsorption, chemisorption or a combination of these properties, influenced by factors such as the chemical structure of the adsorbate and the ionic strength of the solution (electrostatic interaction) [17]; Van der Waals forces, hydrophobic interactions and hydrogen bond formation (non-electrostatic interactions); the size, solubility, degree of dissociation of the substituents and the dipole moment of the sorbate molecules. The electrostatic interaction between the adsorbent and the adsorbate is also significantly influenced by the presence of hydrogen and hydroxyl ions depending on the pH of the solution [18]. The sorption capacity of clay products can be modified by changing the pore volume and specific surface area by addition of different chemical reagents and by selection of different thermal sintering regimes.

The growing population caused requirement for agriculturally and domestically applicable water saving measures leads to increased demand for efficient porous moisture-retaining materials such as lightweight expanded clay aggregates (LECA), which require a high thermal sintering temperature (about 1200 °C) during manufacturing process [19]. The development of highly porous ceramic materials production at low sintering temperatures is one of the efficient ways to support the EU's requirements for reduction in energy consumption and CO_2

emissions. The utilization of glass in the production of such materials contributes to the recycling process, which is one of the most important long-term goals of the EU to achieve a climate-neutral Europe in 2050. Decrease in melting temperature of the ceramic material without reduction in essential physical and mechanical properties of the final product and even by increasing the final density of the matrix microstructure is possible by using glass as melting agent in the clay ceramic composite.

The homogeneity of clay raw materials and additives affects the quality of porous ceramic products. Thus, it is necessary to apply efficient methods of crushing and mixing of dry raw materials. The grinding of materials with significantly different hardness ranges and low impurity content in the final powder characterizes a relatively compact continuous two-rotor disintegrator [20] with up to 10 times lower energy consumption compared to ball mills.

Homogeneous dispersion of different shaped and sized materials (templates) made of combustible and other disappearing (sublimating, evaporating, chemical bonding with ceramic by decreasing volume, etc.) phases followed by drying and thermal sintering allows to produce a highly porous ceramic material with tunable pore sizes and structures [21]. The easy-to-use organic and inorganic disappearing phases [22] pose a number of challenges due to the formation of significant amount of gaseous substances and chemical composition of the final product. The most important of these are the formation of cracks in the matrix; an increase in required energy (and time) consumption for elimination of harmful gaseous substances; as well as the applicability restrictions due to the physical and chemical properties of the final products [16]. The shape of the porous aggregates with a uniform size distribution and good shape repeatability allows the use as the filler in a matrix of another material (for example, in production of lightweight concrete block).

At the same time, there is practically no systematic research in the literature on the possibilities of utilization of glass fragments in Latvian (illite-type carbonate-free) clays, producing highly porous ceramic products. The obtained highly porous ceramic materials can be used as sorbents in water treatment technologies: for binding oil products released into the environment, in building materials as an effective thermal insulation material.

According to the literature review, it can be concluded that almost limited number of reports are available on systematic studies about the effect of glass on the properties of illite clay ceramic materials with the aim to produce porous and highly porous ceramic products at relatively low thermal sintering temperatures (700–1050 °C). It is, therefore, concluded that:

- the addition of glass to the clay powder allows to reduce the required thermal sintering temperature for production of a ceramic material with the required mechanical strength;
- the implementation of sacrificial template method and rotary granulation can provide granulation of clay-glass powder for production of ceramic hollow aggregates (CHA) with open porosity, relatively low required sintering temperature, and relatively high physical and mechanical properties;
- a high-performance disintegrator can be employed for homogenization of a clay-glass mixture with lower required energy consumption;

- rotary-mixer disperser with cavitation effect can be used for preparation of clay-glass suspension and subsequent foaming for production of highly porous clay ceramic foam (CCF) with relatively low required sintering temperature and relatively high final physical and mechanical properties;
- rotary cylindrical granulation device can be used for granulation of foamed clay suspension by using anti-agglomeration agents (e.g., dry clay or peat powder) to obtain highly porous foamed clay granules (FCA) with low required sintering temperature and relatively high final physical and mechanical properties.

2. EXPERIMENTAL

The full experimental process of this Doctoral Thesis, including analysis methods and results obtained in three basic stages, are schematically shown in Fig. 2.1.

In the first stage, *Liepa* clay and milled bottle glass dry mixtures with 0 wt. %, 5 wt. %, 7 wt. %, 10 wt. %, 13 wt. %, and 15 wt. % of glass content were obtained. The materials were analysed both thermogravimetrically (20 °C to 1100 °C, *Derviatograph 1000*) and as semi-dry mass extruded cylindrical samples (1) in Fig. 2.1 and were studied after firing at 700 °C, 800 °C, 900 °C, and 1000 °C.

In the second stage, manufacturing methods for porous clay composite structures were investigated and improved. The physical-mechanical properties of the materials were also evaluated. Porous clay ceramics were obtained following three procedures: 1) the sacrificial template method using different concentrations of glass-containing ceramic hollow aggregates (CHAs; (2) in Fig. 2.1) using a self-made rotary cylindrical granulation machine; 2) clay ceramic foam (CCF) in the form of a prism ((3) in Fig. 2.1), obtained by the direct foaming method using mixer-disperser; 3) and foamed clay aggregates (FCAs), obtained by a combination of the direct foaming and granulation methods mentioned above ((4) in Fig. 2.1), fired at 700 °C, 800 °C, 900 °C, and 1000 °C.

In the third stage, low-temperature clay CHA and FCA prototypes for water retention and chemical sorption were synthesized ((2) and (5) in Fig. 2.1) and investigated. Ceramic hollow granule concrete blocks were used for construction ((3a) in Fig. 2.1) and CCF structures for thermal insulation ((3a) in Fig. 2.1), employing optimized composites and advanced product fabrication techniques in the first stages of operation. Prism-shaped CCF samples, after firing at 900 °C, were used for textile dye adsorption experiments at a zero charge point (pH_{pzc}), ranging from pH 2 to 12 and the effect of the starting dye concentration (10 to 1000 $mg \cdot L^{-1}$) on sorption capacity was evaluated. The FCA obtained by the combined method was used for sorption studies of petroleum-based (petrol, diesel, and motor oil) model solutions, including determination of sorption surface morphology, mechanical strength, specific surface area, porosity, and buoyancy. The water retention abilities of CHA materials fired at 950 °C to 1050 °C were determined by adding 50 cm^3 of the studied material in two model soils, containing, respectively, sand or sand with peat (in a 1:1 weight ratio). All experiments were repeated at least three times.

The following instrumental analysis methods were used in this research: X-ray diffraction (XRD; diffractometer *Panalitical X'Pert PRO*), high temperature microscopy (microscope with heating chamber *EM201, HT163, Hesse instruments*), thermogravimetric analysis, nitrogen adsorption porosimetry by the Brunauer–Emmet–Teller method (BET; sorbtometer *Quadrosorb SI Kr ar Standart Autosorb degasser 5,11*), differential scanning calorimetry, ultraviolet-visible light spectrophotometry (UV-VIS; spectrophotometer *UV-VIS Evolution 300, Thermo scientific*), thermal dilatometry, scanning electron microscopy (SEM; field emission SEM *Tescan Mira/LMU*), and optical microscopy (digital light microscope *Kyence VHX-1000*, with 54 MPx digital camera and *VH-112 Z20R/Z20W* lens).

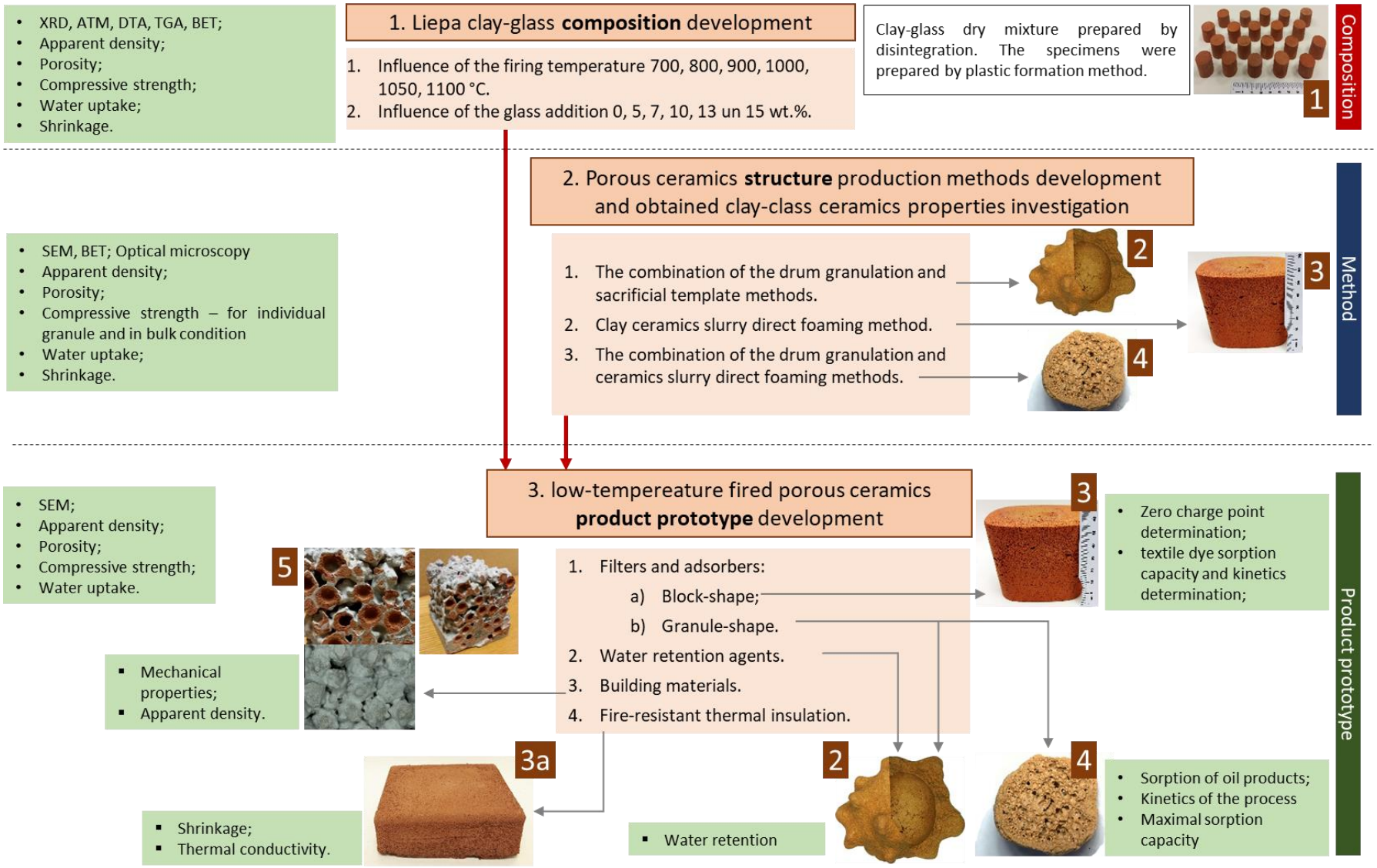

Fig. 2.1. Glass-ceramic material research plan and utilized characterization methods. Material designation: 1– clay-glass composites, 2 – CHA, 3 and 3a – CCF, 4 – FCA, and 5 – CHA-B.

3. RESULTS AND DISSCUSSION

3.1. Effect of Glass Additives on Clay Ceramic Properties

The effect of glass additives on the clay ceramic properties was studied with 0–15 wt. % glass admixture, prepared by extrusion of plastic mass, in the form of cylinders. The obtained samples were dried and, subsequently, fired at 700 °C, 800 °C, 900 °C, and 1000 °C.

3.1.1. Granulometric Composition of the Clay-Glass Batch

This work used a high-intensity disintegrator, *DSL-175*, which is a continuous-action shredder with its operation based on transferring the energy required for milling to the material in the form of impacts, while still providing relatively short residence times of the shredded material in the disintegrator's operating chamber. One-cycle clay disintegration of the studied clay disintegrator leads to a milling ratio (n) of 71 (for ~70 %) and 714 (for ~30 %), yielding a weighted average of $n = 132$ and $n = 10$, respectively, for single-cycle shredding of the cullet. Repeated clay milling results in an increased fine particle size from 30 to 70 % and an increase in the degree of crushing to $n = 260$, yielding two dominant particle sizes, 0.0350 mm and 0.0035 mm, respectively, with a cumulative particle size distribution of 50 % (d_{50}). In the case of repeated glass milling, a relatively homogeneous fraction of the granulometric composition is obtained, with the degree of grinding increasing to $n = 25$ and the corresponding d_{50} decreasing from 0.25 mm to 0.10 mm. The specific power consumption (E_{sp}) for second crushing increases from 2.4 (in one cycle) to 6.8 $kWh \cdot t^{-1}$ (in two cycles).

3.1.2. Structure and Properties of Obtained Clay-Glass Ceramics

Results of differential thermal analysis (DTA) and thermal dilatometry (TG) exhibited two endothermic and one exothermic reaction in all cases. The first endotherm, in the temperature range between 20 °C and 200 °C, is linked to a 2 % relative mass loss in the case of pure clay. This effect indicates the removal of physically adsorbed water (and the rest of the water, which was added during the preparation) and decomposition of crystal hydrates. Hydrocarbon oxidation characterizes the observed exothermic effect between 200 °C and 400 °C. The second dominant endothermic peak is linked to the dehydroxylation of the clay mineral, illite, between 400 °C and 700 °C, accompanied with mass loss. The process causes a decrease in the samples' masses, as the constituent water evaporates. The intensity of the observed effects decreases by increasing the glass concentration. A further increase in glass concentration, up to 15 wt. %, leads to similar intensities in DTA and TG plots, as compared with previous mixtures (5 wt. %).

The phase composition of the studied samples below 800 °C showed a gradual increase in the amorphous content with glass content in the mixtures. Above 800 °C, the mineral illite underwent structural collapse, and a glassy phase formed, in accordance with results reported for clay with high illite content. Owing to this transition, the amorphous content increased further. After heating at 1000 °C (without glass addition), quartz, muscovite, illite, diopside, haematite, and microcline mineral phases were identified in the sample (Table 3.1). Glass addition gives rise to a new mineral phase, as cristobalite appeared in the fired samples. At

temperatures above 960 °C, silica tends to form cristobalite, explaining the increase in cristobalite content with temperature [24]. On the other hand, glass addition led to a decrease in quartz content after the highest firing temperature. Comparing samples with 0 wt. % and 15 wt. % glass addition, some mineral phases evidently vanished (notably, magnetite). Diopside formed at lower temperatures (800 °C) and in higher amounts, while only cristobalite appeared as a new mineral phase. The amounts of crystalline phases and the total degree of crystallinity are represented in Table 3.1 The amount of each crystalline phase was calculated from only the crystalline portions (amorphous phases were excluded). Clearly, glass addition, rather than increasing amorphous content, supports crystallization at high temperatures.

Table 3.1

Phase Composition of Fired Clay and Clay-glass Ceramics

Phase, %	**Glass cullet loading**										
	0 wt. %					15 wt. %				100 wt. %	
	20 °C	700 °C	800 °C	900 °C	1000 °C	700 °C	800 °C	900 °C	1000 °C	20 °C	1000 °C
Quartz	40.8	60.9	60.3	71.0	72.6	58.7	57.7	69.1	67.9		
Illite	45.8	29.2	28.7	18.5		33.8	25.9	6.8			
Haematite	3.1	1.5	1.8	3.0	5.3	3.6	5.3	5.0	4.6		
Microcline	3.4	7.9	8.7	7.1	8.3	3.9	5.6	6.8	8.6		
Kaolinite	6.9										
Magnetite		0.51	0.49								
Diopside					1.7		5.5	4.8	5.3		60.4
Spinel					12.2			3.9	7.3		
Cristobalite								3.5	6.4		
Wollastonite											39.6
Amorphous phase	13.0	13.0	14.0	21.0	26.0	16.0	15.0	21.0	26.0	100	85.0

Thermal dilatometry measurement of clay-glass compositions and compressive strength curves are shown in Fig. 3.1. Based on these results, the onset of sintering for the studied clay powder was at 900 °C, and the onset of densification of the studied glass occurred at about 550–600 °C, with subsequent *Littleton* softening at 716 °C, which is associated with a decrease in glass viscosity to 6.6 $Pa \cdot s^{-1}$ [13], [25]. Glass densification ceased at 900 °C with subsequent liquid phase formation, causing glass expansion from 900 °C to 1000 °C. Further decreased glass velocities were observed upon further increasing the temperature. Addition of glass to the clay ceramic, from 5 wt. % to 15 wt. %, resulted in a similar reduction in sintering temperature for all composites from 900 °C (clay) to 860 °C, demonstrating that the addition of glass acts as a clay sintering promoter. The studied ceramic materials have a fragile nature, i.e., there is practically no plastic deformation prior to destruction. The compression strength value of the studied clay-glass compositions increases rapidly at firing temperatures above 800 °C, and a significant increase in strength is observed for ceramic samples containing more than 10 wt. % of glass after sintering above 900 °C, reaching up to 240 MPa after burning 15 wt. % of glass-containing ceramics at 1000 °C.

Water absorption of the studied glass-containing ceramics decreases intensely from approximately 21 % to 13 % upon increasing the firing temperature in the range of 800 °C to 1000 °C, demonstrating the intense onset of sintering and the formation of closed pores at

900 °C. Increasing the temperature in this interval also reduces the apparent porosity of the clay pottery from 35 % to 24 % and increases the apparent density from 1.68 g·cm^{-3} to 1.92 g·cm^{-3}, as shown in Fig. 3.1 b). Adding up to 5 wt. % of glass reduces the apparent porosity of the ceramic material and water absorption by at least 6 % and 4 %, respectively. Increasing the glass concentration increases the apparent density of the material by ~10 %. The apparent porosity of all samples, with a glass content above 10 wt. %, decreases below 15 % after firing at 1000 °C. Increasing the glass concentration, up to 15 wt. %, reduces water absorption of the clay pottery by factors of two (after firing at 700 °C) and three (after firing at 900 °C).

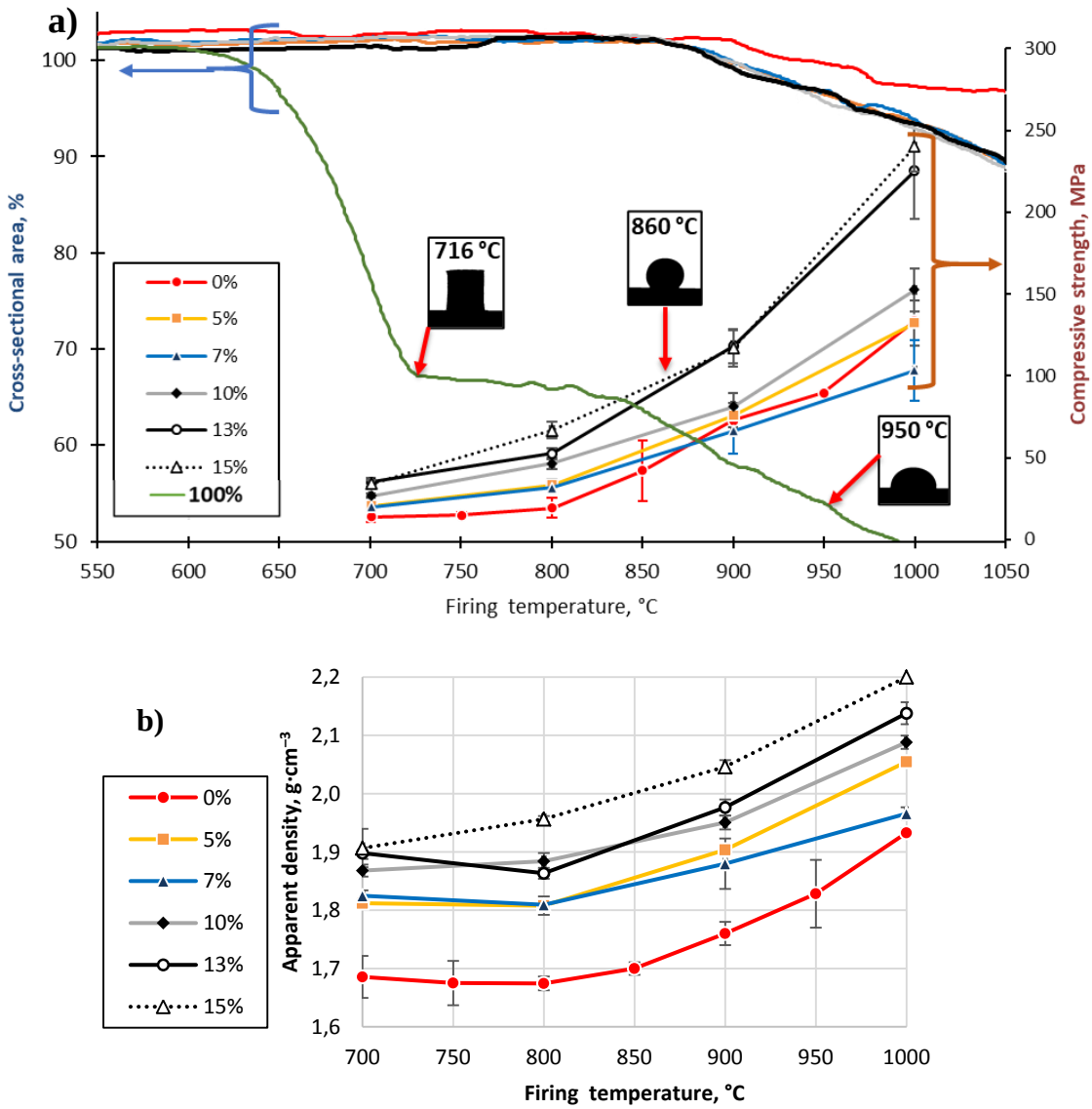

Fig. 3.1. Influence of glass addition on the clay ceramic during firing: a) dilatometric curves of the tested clay-glass ceramic materials from 20 °C to 1050 °C (left *y*-axis) and compression strength (right *y*-axis); and b) apparent porosity of fired clay-glass ceramics with sintering temperature.

Clay is characterized by thermal shrinkage, which is defined as the reduction of linear dimensions as a result of physico-chemical processes. The addition of glass additives reduces the shrinkage of ceramic products by an average of 2 % to 4 %, depending on the firing temperature.

By applying the determined physico-mechanical properties of the obtained samples to M. F. Ashby's strength compression and density summary diagram [26] (Fig. 3.2), we can conclude that the obtained material is characterized by relatively low density and high strength ceramic characteristics, which is one aim of this work.

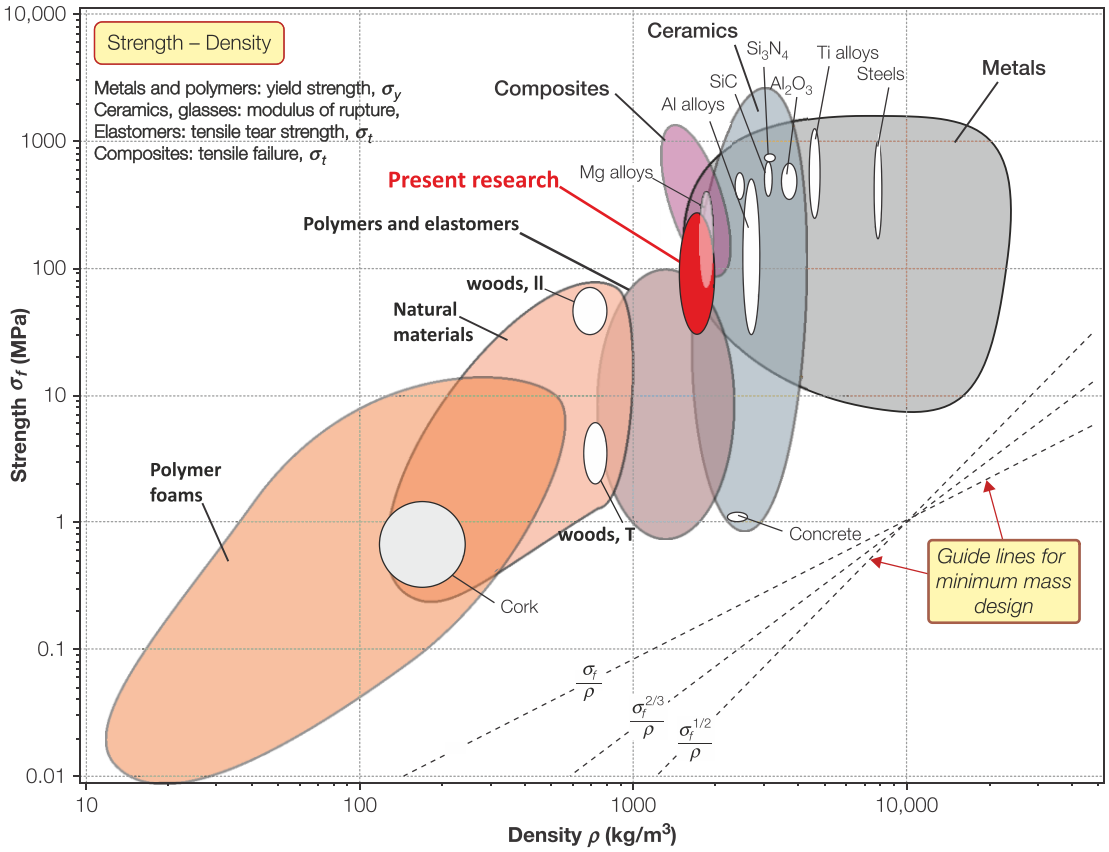

Fig. 3.2. Influence on the compliance of produced clay-glass ceramic materials compared with typical materials, shown in the Ashby classification diagram (adapted from [26]).

3.2. Obtaining Ceramic Hollow Granules and Their Properties

The studied clay-glass compositions were used to obtain CHAs, with the aim to expand possibilities using clay. CHA was obtained by the sacrificial template method using expanded polystyrene (EPS) as a template in a rotary-type granulator.

CHA quality depends on several granulation parameters, in particular the rotational speed of the drum granulator. This value should be selected so that intensive rolling of granular materials takes place without exceeding the critical rotation speed calculated in this work (n_{kr} = 104 min^{-1}) and approved by experiments (n_{kr} = from 95 min^{-1} to 100 min^{-1}). The resulting CHA was characterized by an average diameter in the range of 5.5 mm to 8.8 mm and average wall thicknesses between 0.65 mm and 0.85 mm, as shown in Fig. 3.3 a and b. The surface of CHA differs from a spherical surface, with rounded protrusions between 0.8 mm and 1.5 mm in height from the surface of the assumed external diameter of the CHA sphere. Visually, the observed CHA shape is not significantly affected by the selected firing temperature regimes or glass concentrations added.

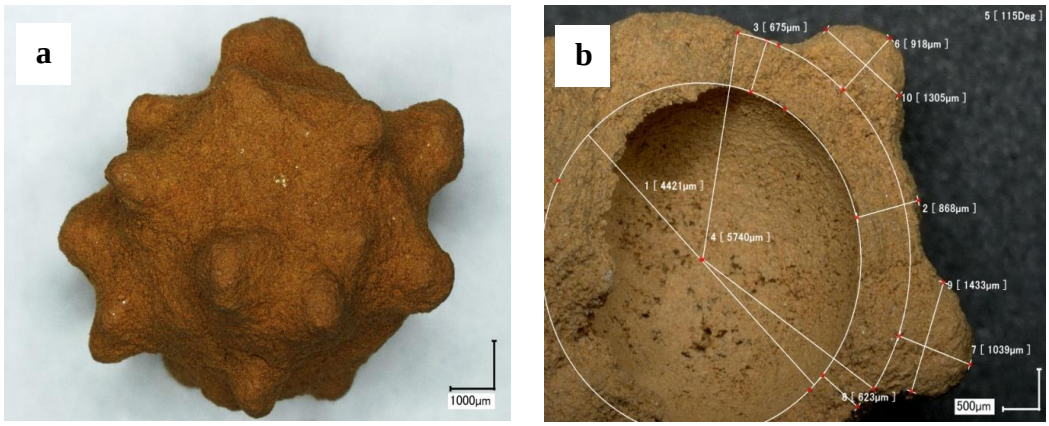

Fig. 3.3. CHA obtained from a drum granulator and sacrificial template method at 1000 °C: a) common view (optical micrograph, 20× magnification) and b) cross-section (optical micrograph, 50× magnification).

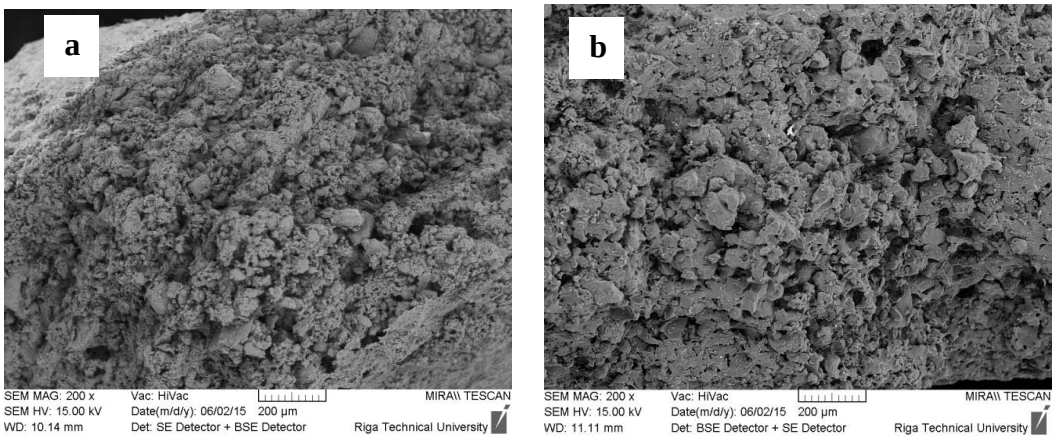

Fig. 3.4. SEM images of CHA wall cross sections, 200× magnification: fired at a) 800 °C and b) 1050 °C.

Increasing the firing temperature from 950 °C to 1150 °C reduces both the porosity of clay CHA (without glass addition), from 66 % to 21 %, and water absorption, from 101 % to 15 %. The onset of intensive clay sintering results in a 2-fold and ~3-fold decrease in apparent porosity and water absorption of clay CHA, respectively. Increasing the temperature from 950 °C to 1100 °C does not significantly affect the apparent CHA (1.50 $g \cdot cm^{-3}$ to 1.59 $g \cdot cm^{-3}$) and bulk densities (0.55 $g \cdot cm^{-3}$ to 0.56 $g \cdot cm^{-3}$). These values increase significantly to 1.66 $g \cdot cm^{-3}$ (apparent density) and 0.70 $g \cdot cm^{-3}$ (bulk density) after firing at 1150 °C, characterizing the reduction in CHA size caused by liquid phase formation. The BET method has shown that increasing the firing temperature from the lowest to the highest value during the studied interval reduces the specific surface area of the clay CHA wall (from 1.907 $m^2 \cdot g^{-1}$ to 0.223 $m^2 \cdot g^{-1}$). These values are drastically reduced in the firing temperature range of 1050 °C to 1150 °C.

The obtained CHA, with glass contents of 5 wt. %, 7 wt. %, 10 wt. %, and 13 wt. %, are characterized by specific surface areas of 10.77 $m^2 \cdot g^{-1}$, 14.51 $m^2 \cdot g^{-1}$, 13.77 $m^2 \cdot g^{-1}$, and 11.00 $m^2 \cdot g^{-1}$, respectively, after firing at 800 °C. Increasing the firing temperature to 900 °C and 1000 °C significantly reduces the surface areas of all studied CHAs from 1.57 $m^2 \cdot g^{-1}$ to

1.12 $m^2 \cdot g^{-1}$ and 0.28 $m^2 \cdot g^{-1}$ to 0.21 $m^2 \cdot g^{-1}$, respectively. The mechanical compressive strength of the poured CHA samples varies from 0.8 MPa to 1.1 MPa, increasing the glass content to 10 wt. % and 13 wt. % after firing at 800 °C, as shown in Fig. 3.5. Increasing the firing temperature to 900 °C and 1000 °C significantly increases the mechanical compressive strength of all CHAs from 0.22 MPa to 0.38 MPa and 0.30 MPa to 0.49 MPa, respectively. Increasing the firing temperature to 1050 °C yields a decrease in the mechanical compressive strength of CHA relative to samples fired at 1000 °C in the range of 0.27 MPa to 0.4 MPa, while maintaining the characteristic overall compressive strength values by increasing the glass content within the studied range.

Due to the properties of CHA, such as its relatively high specific surface area and sufficient mechanical strength, a sorbent with ferromagnetic properties was developed in this work. In addition to clay and glass, iron powder or industrial waste – slag (a mixture of iron oxides, e.g., Fe_3O_4, Fe_2O_3, and FeO) – was added to the composition, providing ferromagnetic properties to CHA. The concept of a ferromagnetic sorbent and the method of obtaining it were approved by a Latvian patent (LV14822B, June 20, 2014). However, the obtained product and its properties were not studied any further within the framework of this Doctoral Thesis.

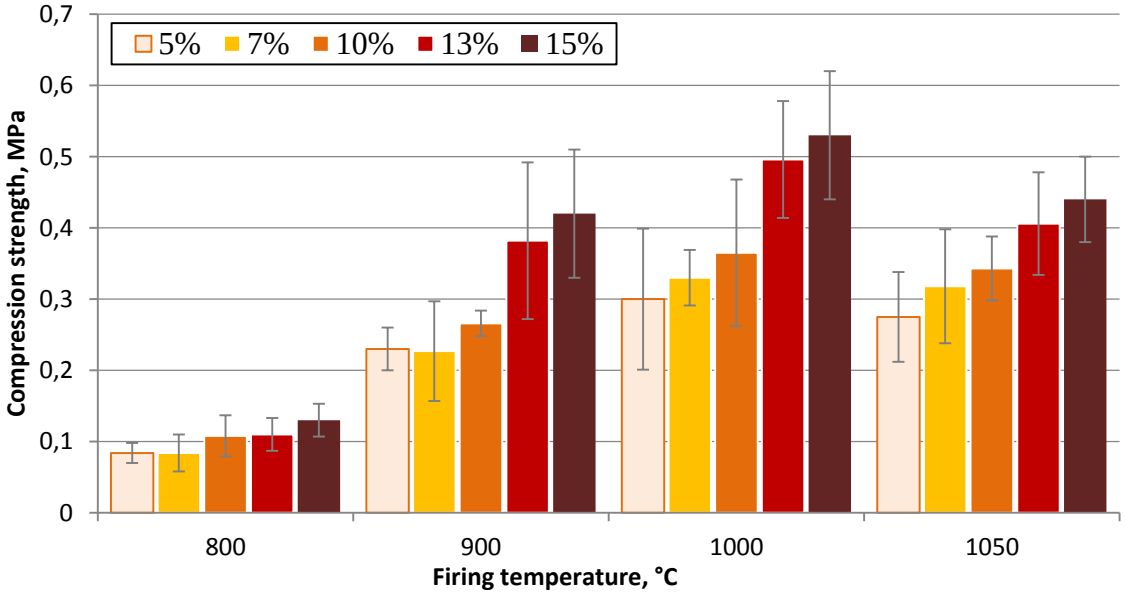

Fig. 3.5. CHA compressive strength in bulk, depending on glass concentration and firing temperature.

One possible application for the obtained CHA pellets is the production of building blocks, replacing expanded clay pellets, which are no longer produced in Latvia. Through experimentation, a technologically optimal recipe was created by dividing the amount of water required for the concrete mix into two parts before mixing. One part was used to moisten CHA, and the other part was mixed into the cement mortar, with a total water-cement ratio (W/C) of 0.9. Specimens matured for 28 days were used for tests. For the production of CHA concrete blocks (CHA-B), CHA containing 0 wt. % to 15 wt. % glass admixture and an average size 8 mm ± 2 mm was selected after firing at 900 °C. Commercial (*Keramzits, Belorussia*) LECA-concrete (KERB) samples, using the same concrete recipe, were obtained,

for comparison. Mechanical compressive strength and bulk density for the prepared samples are shown in Fig. 3.6. Replacement of *Kermzite* with CHA increases the strength and bulk density of the block by 37 % (reaching 4.9 MPa) and 15 % (841 kg·m^{-3}), respectively. The addition of glass, up to 7 wt. %, increases the compressive strength and bulk density of CHA-containing blocks to 7.1 MPa and 1070 kg·m^{-3}, respectively. A further increase in the glass concentration causes a decrease in compressive strength of the CHA block to 4.0 MPa and a decrease in bulk density to 841 kg·m^{-3}. This effect can be explained by intensification of clay sintering, caused by glass, and the consequent decrease in porosity, which results in a lower cement mortar absorption capacity in the porous structure of the ceramic. As a result, the total compressive strength of CHA-B also decreases, despite the fact that the compressive strength of individual CHA increases with increasing glass content.

Visual observations confirm the hypothesis that the specific shape of CHA can provide greater mutual adhesion and more efficient fixation (reinforcement) in a matrix of another material than spherical type granules, as shown in Fig. 3.6 b and c. Further, CHA and cement mortar were found to bind relatively well. This effect can be explained by the penetration of cement mortar into the porous walls of CHA. In the case of expanded clay concrete block (KER-B), diffusion of cement solution in expanded clay aggregates is observed significantly less than with CHA. This effect is due to the higher open porosity of CHA compared to expanded clay.

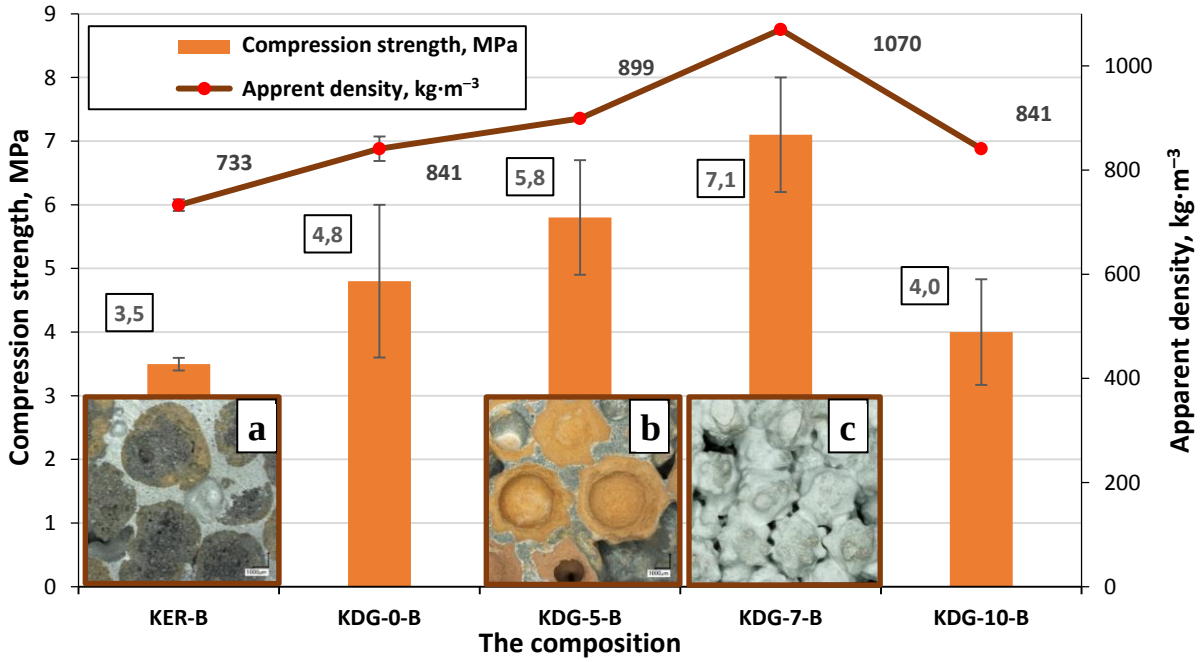

Fig. 3.6. Compressive strength and bulk density of KER-B and CHA-B samples containing 0 wt. %, 5 wt. %, 7 wt. %, and 10 wt. % additives (designated as KER-B, CHA-5-B, CHA-7-B, and CHA-10-B) fired at 900 °C. Optical microscopy images show cross-sectional images for the placement of granules in the expanded clay-concrete block (a) and a CHA-concrete block (b), as well as a surface image of the CHA-concrete block (c).

3.3. Production and Properties of Highly Porous Glass-Containing CCF

Recently, highly porous ceramic materials are attracting more and more attention. CCF from the clay-glass water slurry were obtained in the work using the direct foaming method in a rotary disperser-cavitator. Clay glass with 0 wt. %, 5 wt. %, 7 wt. %, and 10 wt. % glass compositions were selected to form a clay slurry, and the resulting foamed slurry was dried in moulds and fired at temperatures from 900 °C to 1050 °C. Intensive shrinkage and crack formation were observed in CCF samples without glass additives. Further, the addition of coarser glass grains resulted in thinning of the ceramic mass, which prevents the formation of cracks in the samples during drying, while maintaining shape stability. The clay-glass compositions studied in this work provide highly porous fired ceramics. Therefore, in this work, CCF materials obtained from clay-glass batch compositions were studied.

3.3.1. Physico-Mechanical Properties of the CCF

The obtained CCF samples were evaluated for their mechanical strength. Their compressive strength increased with increasing firing temperature from 900 °C to 1050 °C. The fastest increase in compressive strength from 3.8 MPa to 14.3 MPa was observed in CCF containing 5 wt. % glass additive (Fig. 3.7).

Binding of clay particles to higher glass concentrations at firing temperatures from 950 °C to 1050 °C resulted in a less intense increase in CCF compressive strength, from 5.8 MPa to 11.1 MPa (7 wt. %) and 3.5 MPa to 6.3 MPa (10 wt. %). This effect is due to the collapse of the less durable amorphous phase in the CCF structure under the applied load.

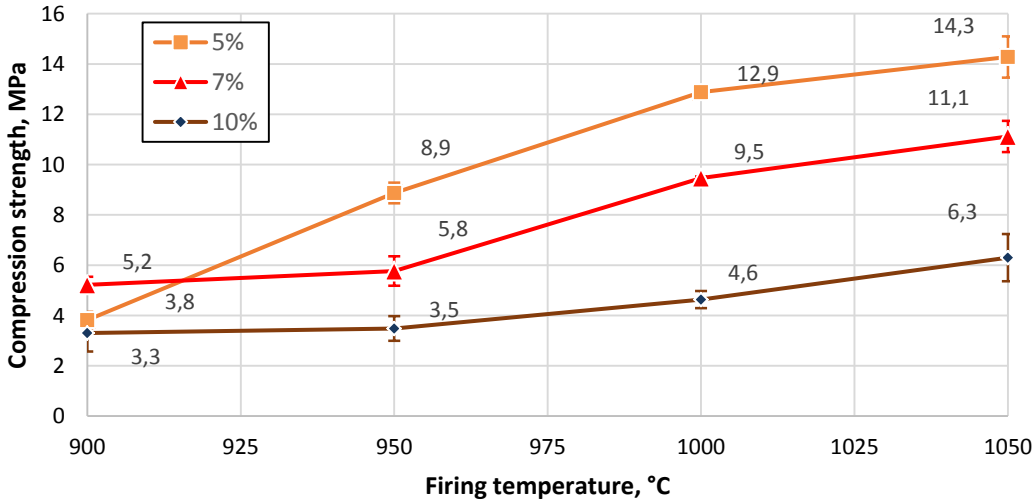

Fig. 3.7. Dependence of CCF compressive strength on firing temperature and glass content.

When determining the open porosity of CCF samples by the Archimedes method, 3–4 % increases of porosity, on average, are observed with increasing glass additive concentrations from 5 wt. % to 10 wt. % at all firing temperatures (Fig. 3.8). Maximum porosity is observed for samples containing 10 wt. % of glass. Compared with dense clay-glass ceramic material, the opposite trend is observed for CCF. Increasing the roasting temperature by 50 °C reduces the

CCF open porosity by 2–3 %, on average. During homogenization and foaming of the slurry, the pores generated by air bound in the disperser-cavitator are evenly distributed in the material, and their average size ranges from 20 μm to 120 μm (Fig. 3.8 a). When the samples are fired, water is removed, organic impurities are burned out, and sintering takes place, as a result of which the material compacts and pore size decreases. At the same time, as shown in Fig 3.8 b, the pore support structure is distinctly porous, with an average pore size of about 1 μm.

Similar to porosity, the apparent density and water absorption properties of CCF samples have the opposite tendencies compared to the dense material. Samples containing 5 wt. % glass show the highest apparent density (average 0.84 $g \cdot cm^{-3}$), and samples with 10 wt. % glass have an average density of 0.71 $g \cdot cm^{-3}$. Increasing the firing temperature increases the density, slightly, to 0.9 $g \cdot cm^{-3}$ (5 wt. %) and 0.75 $g \cdot cm^{-3}$ (10 wt. %).

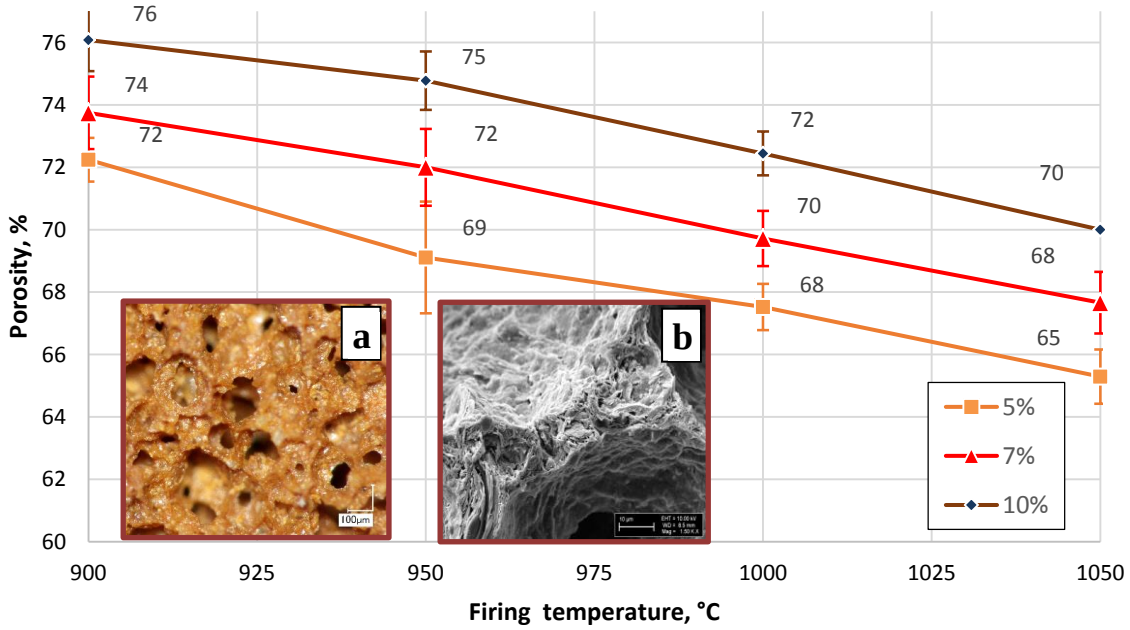

Fig. 3.8. Dependence of CCF porosity on firing temperature and glass content: (a) optical microscopy of the pore structure and (b) SEM images of the pore support structure.

Glass additives promote water absorption capacities of foam ceramics. The highest water absorption (up to 122 %) was observed for samples containing 10 wt. % glass additive, fired at 900 °C. The specific surface area ($m^2 \cdot g^{-1}$) was determined for the samples obtained by firing at 900 °C, 950 °C, and 1000 °C. Increasing the roasting temperature from 900 °C to 950 °C reduces the specific surface area of CCF by an average of 4–5 times (from 2.8 $m^2 \cdot g^{-1}$ at 900 °C to 0.6 $m^2 \cdot g^{-1}$ at 950 °C), which is related to the above processes during firing.

The high porosity and water absorption capacity obtained for CCF are promising toward its use in water treatment technologies. Therefore, the sorption capacity of organic substances was studied.

3.3.2. CCF Sorption Properties

The obtained foamed clay ceramic, with relative porosity up to 80 %, is characterized by a relatively high mechanical strength and could potentially be used as a sorbent in wastewater

treatment in the textile industry, for example. Therefore, the sorption properties of CCF were studied using the textile dye *Bezaktiv Turquise Blue V-G* (BTB) as a model sorbate. Ceramic samples with 10 wt. % glass content after sintering at 900 °C were used for sorption studies.

To estimate the optimal sorption conditions, the pH zero charge point (pH_{NLP}) was determined for the studied samples, and the value of pH_{NLP} = 6.16 was determined in the present work. Therefore, BTB is an anionic dye, and the best sorption capacity is expected in an acidic environment. In fact, the maximum sorption capacity was observed at pH = 2, and all sorption experiments were performed at this pH value, adjusting the BTB concentration in the solution to 50 mg·L^{-1}, 100 mg·L^{-1}, or 200 mg·L^{-1}.

The increase in BTB dye concentration in the solution increases the achievable values of adsorption equilibrium, as well as the time required to reach equilibrium, as demonstrated in Fig. 3.9 a. Various kinetic models can be used to elucidate the limiting stages and mechanism of the adsorption process. The Weber–Morris diffusion model is commonly used to separate effects of external and internal diffusion of adsorbates on the adsorption process, which is mathematically described by Equation (3.1) [27].

$$q_t = K_{id} t^{0.5} + C, \quad (3.1)$$

where q_t is the amount of the adsorbed BTB, mg·g^{-1}; K_{id} is the Weber–Morris constant, or internal diffusion rate constant, in the pores, mg·g^{-1}·min$^{0.5}$; and C is constant parameter related to the boundary layer thickness, mg·g^{-1}. Two stages of the sorption process are clearly distinguished in the coordinates q_t–$t^{0.5}$ for all initial BTB concentrations in the model solution (Fig. 3.9 b). The first stage q_t–$t^{0.5}$ characterizes the limiting effect of external diffusion, and the second relates more to diffusion of the adsorbate through the boundary layer and in the adsorbent pores [28]–[30].

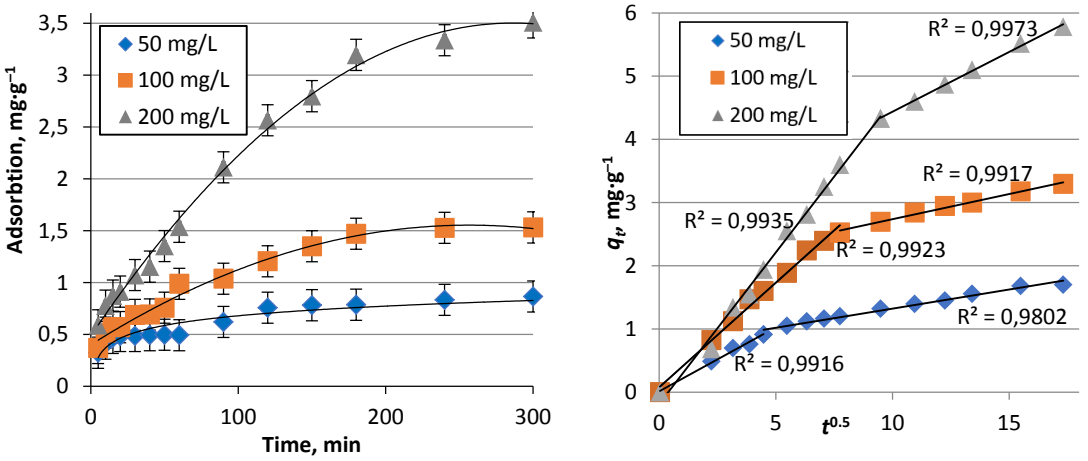

Fig. 3.9. Sorption kinetics (a) and representation of the adsorption process in q_t–$t^{0.5}$ coordinates, depending on the initial concentration of BTB (b) for ceramic foam sample with 10 wt. % of glass and fired at 900 °C.

The kinetics of the adsorption process on a solid sorbent surface is often characterized by pseudo-first and pseudo-second order kinetic models. The pseudo-first order adsorption kinetics are used to characterize the adsorption process at the solution-solid interface [31]. Kinetic Equation (3.2), of the following model, describes the sorption capacity of the sorbent [32], [33]:

$$\frac{\mathrm{d}q_t}{\mathrm{d}t} = k_1(q_\mathrm{e} - q_t), \tag{3.2}$$

where q_t is the amount of adsorbed dye during time t, mg·g^{-1}; q_e is the amount of adsorbed dye at steady state, mg·g^{-1}; and k_1 is the pseudo-first order model adsorption rate constant, g·mg^{-1}·min^{-1}; while t describes the duration of adsorption, min.

In addition to the influence of diffusion processes, the pseudo-second order kinetic model also evaluates the influence of possible reactions in the sorbent-sorbate system [33], [34]. The classical form of the pseudo-second order kinetic model is (3) [31]:

$$\frac{\mathrm{d}q_t}{\mathrm{d}t} = k_2(q_\mathrm{e} - q_t)^2, \tag{3.3}$$

where k_2 is the constant of the pseudo-first order model, g·mg^{-1}·min^{-1}.

Linear forms of Equations (3.2) and (3.3) were used to analyse the sorption process. The linear expressions and process parameters [35] of the adsorption kinetic models are shown in Table 3.2.

Table 3.2

Adsorption Kinetic Models, Linear Expressions, and Parameters

Kinetic model	Linear expression of the equation	Variables	Parameters
Pseudo-first order	$\ln q_t = \ln k + v\ln t$	$y = \ln(q_\mathrm{e} - q_t)$; $x = t$	k = exp(intersection with the axis); v = direction factor
Pseudo-second order	I Type $t/q_t = 1/(k_{2\mathrm{p}}\, q_\mathrm{e}^2) + t/q_\mathrm{e}$	$y = t/q_t$; $x = t$	q_e = (coefficient of the direction)$^{-1}$; $k_{2\mathrm{p}} = q_\mathrm{e}^2$ / intersection with the axis
	II Type $1/q_t = 1/[(k_{2\mathrm{p}}q_\mathrm{e}^2)(1/t)] + 1/q_\mathrm{e}$	$y = 1/q_t$; $x = 1/t$	q_e = (intersection with the axis)$^{-1}$; $k_{2\mathrm{p}} = q_\mathrm{e}^2$ / direction factor

The kinetic equation parameters are calculated from the obtained relations. As seen from Table 3.3, the BTB adsorption process on CCF sorbents is most accurately described by the pseudo-second order type I kinetic model (R^2 values ranging from 0.914 to 0.990). In addition, the experimentally determined and calculated adsorption equilibrium values are sufficiently close. According to this model, we can conclude that the adsorption process takes place in a mixed diffusion mode and can be influenced by the interaction of BTB and active sorbent centres.

In sorption processes, equilibrium data are usually represented in the form of sorption isotherms. The isothermal form reflects the intensity of the adsorption process and interaction between the adsorbate and adsorbent. Representing experimental data on the achieved

equilibrium in the sorption processes, an adsorption isotherm was obtained (Fig. 3.10), which, according to Braunauer classification [36], most likely corresponds to type I or II isotherms.

Table 3.3

Kinetic Parameters of BTB Adsorption Models on the Surface of CCR, with 10 wt. % of Glass

Initial conc.	Q_e, mg·g^{-1} exp.*	Pseudo-first order			Pseudo-second order type I			Pseudo-second order type II		
		k_2, g·mg^{-1}min^{-1}	q_e, mg·g^{-1}	R^2	k_2, g·mg^{-1}min^{-1}	q_e, mg·g^{-1}	R^2	k_2, g·mg^{-1}min^{-1}	q_e, mg·g^{-1}	R^2
50	0.845	0.01	0.529	0.945	0.067	0.881	0.990	0.111	0.846	0.781
100	1.529	0.02	1.750	0.892	0.016	1.684	0.969	0.055	1.279	0.782
200	3.423	0.01	3.535	0.975	0.004	4.01	0.914	0.022	2.397	0.787

* experimental data.

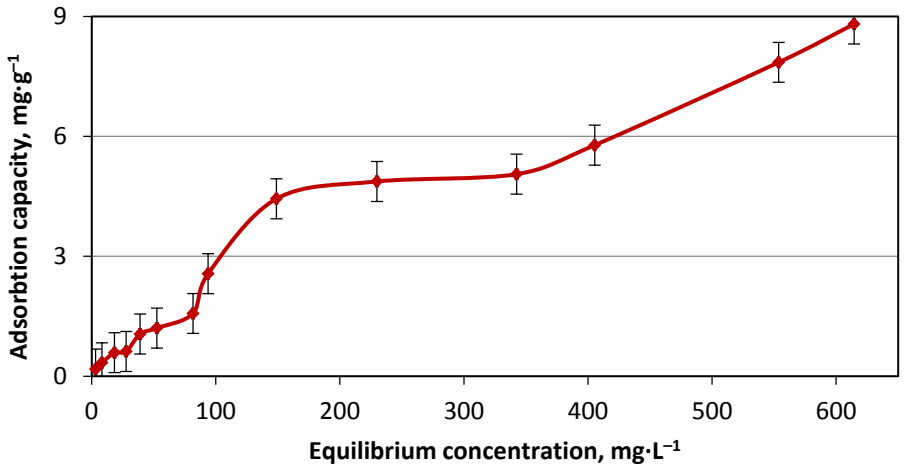

Fig. 3.10. BTB sorption isotherm on the surface of a sample with 10 wt. % of glass, fired at 900 °C.

Langmuir and Freundlich theoretical adsorption models were used to characterize the adsorption isotherms obtained in references [31], [37], [38]. Most often, these models and their corresponding equations are represented in linear form [39] (Table 3.4).

Table 3.4

Linear Expressions and Parameters of Adsorption Models

Isotherm model	Linear expression of the equation	Variables	Parameters
Freundlich	$\ln q_e = \ln K_F + n^{-1}\ln C_e$	$y = \ln q_e$; $x = \ln C_e$	K_F = exp(axis crossing); n = (direction coefficient)$^{-1}$
Langmuir	(II) $1/q_e = 1/(K_L q_m C_e) + 1/q_m$	$y = 1/q_e$; $x = 1/C_e$	q_m = (axis crossing)$^{-1}$; K_L = direction coefficient

where q_e is the amount of adsorbed substance, mg·g^{-1}; q_m is the maximum monolayer capacity, mg·g^{-1} C_e is the adsorbate concentration in the solution at equilibrium, mg·L^{-1}; K_L is the Langmuir constant; and K_F and n^{-1} are Freundlich constants, which characterize the adsorption capacity and intensity, respectively.

The linear forms of the Langmuir and Freundlich equations were used to describe the obtained adsorption isotherms. These models properly describe experimentally obtained BTB sorption data, which is evidenced by high determination coefficients ($R^2 > 0.95$). The calculated constants of the Longmuir and Freundlich theoretical equations and the maximum sorption capacity ($mg \cdot g^{-1}$), in the case of the Langmuir equation, is shown in Table 3.5. As seen, the CCF sorption capacity ($q_m = 3.16\ mg \cdot g^{-1}$), calculated according to the Langmuir model, is less than the experimentally obtained value (Fig. 3.10). This confirms the above described assumption regarding the complex nature of the sorption process. Apparently, at the beginning of the process, sorption to sorbent active centres dominates, and bound BTB molecules serve as new adsorption centres at the same time. This assumption is also indirectly confirmed by the Freundlich isotherm constant, $n = 0.855$, which indicates a possible chemical interaction between sorbate molecules and active centres on the CCF surface.

Table 3.5

Parameters of the Obtained Sorption Isotherm Theoretical Models

Adsorption model	R^2	Parameters
Langmuir	(II) 0.956	$q_m = 3.16\ mg \cdot g^{-1}$; $K_L = 0.018\ L \cdot mg^{-1}$
Freundlich	(II) 0.980	$K_F = 0.065\ mg \cdot g^{-1}$; $n = 0.855$

R^2 – values of coefficients of determination; q_m – maximum monolayer capacity; K_L – Langmuir constant.

3.3.3. CCF for Improvement of Building Blocks' Thermal Insulation Properties

The EU is assigning increased importance to reducing energy consumption. Energy Efficiency Directive 2012/27/EU [14] required member states to reduce their energy consumption by 20 % by 2020. To improve the energy efficiency of new residential buildings, cellular ceramic building blocks have been used extensively in construction. They are characterized by a certain shape of vertical channels. In the Baltic region, well-known *Keraterm* blocks (*AS Lode*, Latvia) have thermal conductivity coefficients (λ) ranging from 0.2 $W \cdot m^{-1} \cdot K^{-1}$ to 0.3 $W \cdot m^{-1} \cdot K^{-1}$ [15]. Nevertheless, ceramic blocks on the market do not meet the growing energy consumption requirements for consumer buildings with almost zero energy consumption in their construction.

The thermal insulation properties of such blocks are summed from the heat conduction phenomena in the channel walls and heat convection in the channel void. Heat transfer in the form of heat convection is the biggest disadvantage of *Keraterm* blocks. However, filling block channels with expanded perlite [40] or other materials obtained from a cement slurry with added foaming agent [41] is a known technique for improving the thermal insulation properties of these blocks.

A new method has been developed to improve the thermal insulation properties of *Keraterm 17.5* blocks, using the CCF production method with the help of direct foaming in a disperser, as described in Chapter 3.3. The prepared clay-water suspension (95 wt. % clay powder and 5 wt. % crushed glass powder relative to the dry matter content), surfactants, electrolyte, and foaming agent were mixed with a hand mixer and, subsequently, foamed in a disperser. *Keraterm 17.5* blocks were filled with the obtained foamed suspension and were

subsequently dried by slowly increasing the temperature up to 105 °C. The foamed material completely fills the block channels and fits tightly to the walls of the block channels, making heat transfer in the block channels by convection an insignificant heat transfer mechanism.

The average value of the experimentally determined thermal conductivity coefficient for *Keraterm 17.5* was $\lambda = 0.21\ W \cdot m^{-1} \cdot K^{-1}$, and λ did not exceed $0.16\ W \cdot m^{-1} \cdot K^{-1}$ for filled and dried blocks. Thus, with the help of the proposed CCF, the thermal conductivity coefficient of the building block was reduced by about 23 %.

3.4. Foamed Clay-Glass Ceramic Aggregates

3.4.1. The Production and Properties of Foamed Clay-Glass Ceramic Aggregates

In this chapter, the production of foamed clay-glass ceramic aggregates (FCA) from foamed clay-glass slurry, using granulation technological parameters and foam ceramic production methods developed in this work, and the study of their properties is discussed.

Slurry with 10 wt. % of glass additives was used for the production of FCA. The clay slurry was foamed with a disperser (see Chapter 2) and metered through a nozzle into a rotating cylindrical granulator. The dry clay and peat powders were used as anti-agglomeration agents during granulation of FCA. Obtained aggregates were dried and, subsequently, thermally processed at 950 °C and 1050 °C. FCA, coated by clay and peat powders, named FCA-C and FCA-P, correspondingly, were obtained.

The use of dry clay powder results in dense and relatively smooth fragments of FCA-C external shell, with a gradient increase in the distribution of pore sizes from 50 μm up to 300 μm toward the centre of the aggregate. This effect can be explained with intensive migration of water from the centre toward the surface of the aggregate while covering with dry clay powder, causing coalescence of the pores inside the FCA-C, as demonstrated in Fig. 3.11 a.

Thermal processing, from 950 °C up to 1050 °C, leads to decreased pore sizes but without a significant effect on the morphology of the aggregate cross section. Therefore, the selected nature of the anti-agglomeration agent significantly influences the final pore structure of the FCA. Porous structure forms in the whole body of the FCA, as observed with SEM imaging, demonstrated in Figs. 3.12 a and 3.11 b.

An increase in processing temperature from 950 °C to 1050 °C leads to more intensive sintering. A portion of pores converge, and plate-type particles form, with clearly observable inter-plate spaces. Specific surface areas and open porosity decreases with increased thermal processing temperatures from 950 °C to 1050 °C (Table 3.6), yielding particle sintering and shrinkage of ceramic aggregates during thermal processing. The apparent density of FCA increases from $1.50\ g \cdot cm^{-3}$ to $1.56\ g \cdot cm^{-3}$ after increasing the thermal processing temperature from 950 °C to 1050 °C. The replacement of peat powder with a coating of dry clay powder leads to an increase in the apparent density of FCA by 5.5 % and 4.6 % after thermal processing at 950 °C and 1050 °C, respectively.

Fig. 3.11. Optical microscopy images of (a, b) FCA-C and (c, d) FCA-P surfaces (a, c) and cross sections (b, d) after thermal processing at 950 °C.

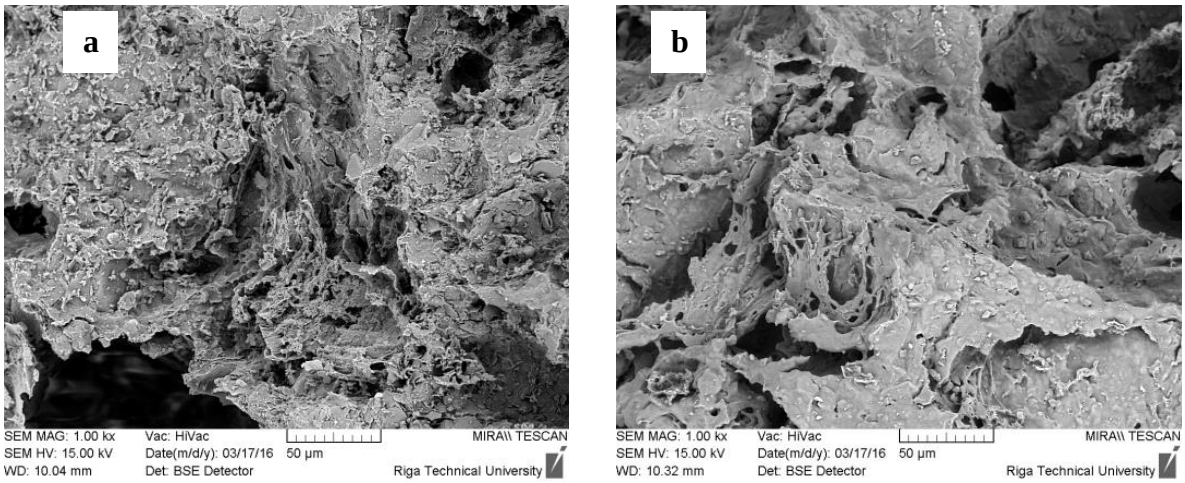

Fig. 3.12. SEM images of FCA-P samples after thermal processing at a) 950 °C and b) 1050 °C.

Table 3.6

FCA-C, FCA-P and CHA (Fired in Temperature Range from 950 °C to 1050 °C) Compression Strength, Specific Surface Area and Open Porosity

Sample	Compression strength, N		Specific surface area, $m^2 \cdot g^{-1}$		Porosity,%	
	950 °C	1050 °C	950 °C	1050 °C	950 °C	1050 °C
PKG-K	11.0 ± 1.5	13.0 ± 2.5	1.98	0.93	74	66
PKG-M	13 ± 2	14 ± 3	1.91	0.90	55	32
KDG	13 ± 2	16 ± 4	1.44	0.49	23	20

3.4.2. Sorption of Oil Products in the Structure of FCA

Foamed clay ceramic produced from the clay suspension with glass additives, by the direct foaming method in a rotary mixer-disperser with a cavitation effect, can be used as dye sorbent for textile industry wastewater. The obtained FCA-P, FCA-C, and CHA (reference sample) specimens were thermally processed at 950 °C and 1050 °C and, subsequently, applied for sorption of oil products (gasoline, diesel, and motor oil). Preliminarily sorption kinetics were estimated for FCA specimens using diesel fuel as a model compound (Fig. 3.13).

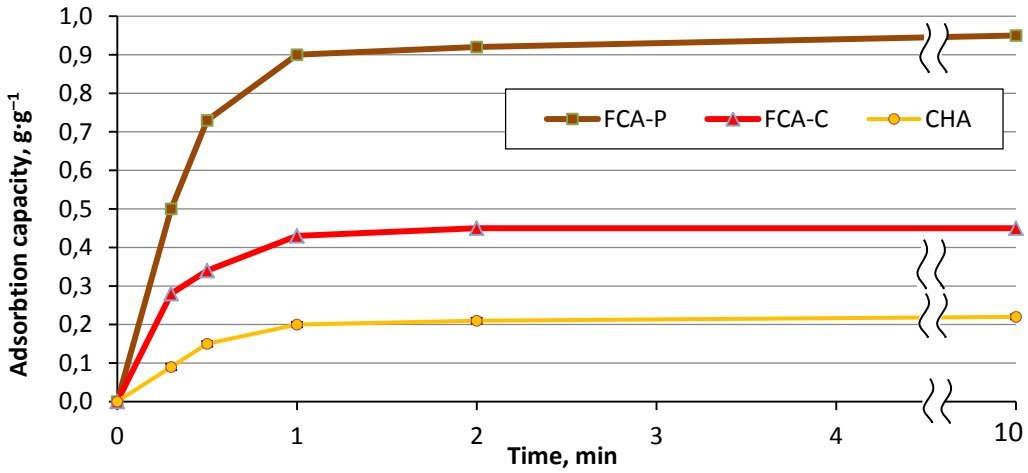

Fig. 3.13. Diesel fuel adsorption kinetics on ceramic aggregate surfaces (FCA-P, FCA-C, and CHA) after thermal processing at 1050 °C.

All experimental results exhibit similar characteristic adsorption kinetic relationships, and all samples reach maximum adsorption capacity in 2–3 minutes. FCA-P exhibits the highest adsorption capacity, as expected due to its high porosity (74 %) and developed external surface. Sorption capacity is two and four times higher for FCA-P compared to FCA-C and CHA, respectively.

An approximated Webber–Morris adsorption kinetical diffusion model was applied to determine the possible oil product absorption mechanisms. Sorbate diffusion rate limits the adsorption rate in adsorbents with a developed pore system (FCA-P) and sufficiently large pore sizes for penetration and arrangement of sorbate molecules at pore walls. The number of adsorbed particles q_τ in period τ is proportional to $\sqrt{\tau}$, and the relationship $q_\tau = f(\sqrt{\tau})$ is linear in this case [27]. The relationship q_τ–$\tau^{0.5}$ in the Webber–Morris equation coordinates is not linear. Two specific areas (stages) were observed, indicating mixed diffusion character of the adsorption kinetics.

The first stage characterizes molecule diffusion from the sorbate volume to the surface of the adsorbent, and the second stage characterizes molecular diffusion in adsorbent pores (mass transfer resulting from internal diffusion). The character analysis of the relation q_τ–$\tau^{0.5}$ leads to the following conclusion: identical sorption characteristics are observed for all specimens (FCA-C, FCA-P, and CHA). FCA-P exhibits the highest oil product sorption capacity, as demonstrated in Table 3.7. The observed sorption capacity ($g \cdot g^{-1}$) increases as

follows: gasoline, diesel fuel, and motor oil, due to the compound densities at 20 °C (0.73 g·cm^{-3}, 0.81 g·cm^{-3}, and 0.83 g·cm^{-3}, respectively).

Table 3.7

Sorption Capacities of Different Oil Products in the Structures of FCA-C, FCA-P, and CHA after Thermal Processing at 950 °C and 1050 °C Temperatures (T_{firing})

Compound	**Gasoline**		**Diesel fuel**		**Motor oil**	
T_{firing}	**950 °C**	**1050 °C**	**950 °C**	**1050 °C**	**950 °C**	**1050 °C**
Specimen	Sorption capacity, g·g^{-1}					
FCA-P	0.83	0.74	0.95	0.93	1.05	0.95
FCA-C	0.38	0.35	0.45	0.43	0.55	0.46
CHA	0.20	0.21	0.22	0.23	0.32	0.20

3.4.3. Water Uptake Capacity in FCA for Soil Moisture Retention

Due to the growing shortage of fresh water on the planet, including that used in agriculture, there is a demand for materials that maintain soil moisture. Due to its relatively large specific surface area and porosity (Table 3.6), FCA could be used to regulate soil moisture.

The model soil (MS), consisting of 92.5 % sand and 7.5 % sieved peat, was used for moisture maintenance experiments. Water uptake capacity of MS was compared with compositions of MS with researched sorbents (MS + FCA-P and MS + CHA), reference specimens with perlite (MS + Perlite), and commercial expanded clay (MS + Ker). The concentration of added sorbents was 30 volume % of the total MS volume.

The content of uptake and maintained moisture was determined experimentally by mixing 150 mL water, 100 cm^3 MS, and 50 cm^3 of researched sorbent, as demonstrated in Table 3.8. The lowest water maintenance (highest loss of water) was observed for MA. Water maintenance can be affected by a wetting phenomenon at the beginning of the test. The water uptake equilibrium was reached in about three minutes in all cases.

Table 3.8

Maintained Moisture in MS and Water Uptake in Sorbents

Parameter	**MS**	**MS + CHA**	**MS + Ker**	**MS + FCA-P**	**MS + FCA-C**	**MS + Perlite**
M_{soil} + M_{sorb}, mL	105	107	112	116	118	127
M_{sorb}, mL	–	2	7.5	11	13	22
M_{sorb}, mL·cm^{-3}	–	0,04	0.15	0.22	0.26	0.44

As seen in Table 3.8, foamed perlite granules have greater water retention ability, which is a relatively expensive and imported material. At the same time, FCA obtained from peat coating has 12 % better moisture retention compared to MA without the addition of moisture retaining materials and 73 % better retention compared to the widely-used expanded clay (MS + Ker).

3.5. Technological Scheme for the Production of Developed Porous Ceramics

The experimental results obtained during doctoral research were used for the development of a technological scheme and balanced for the production of developed ceramic materials.

3.5.1. Crushing of Raw Materials and Batch Preparation Scheme

Delivered raw materials were prepared with the help of equipment pieces (1)–(8), shown in Fig. 3.14. Clay (1) and glass cullet (2) inserted in the roller crusher (3) and, subsequently, in the hammer crusher (4) were crushed to particles with sizes less than 25 mm. Crushed raw materials feed into the continuously operating disintegrators (5) and (6), yielding particles with sizes from 0.1 mm to 1.0 mm. The specific electrical energy consumption of the disintegrator is E_{sp} = 2,4 kWh·t^{-1}, and d_{50} values of the obtained crushed glass and clay particles are 0.25 mm and 0.1 mm, respectively, as experimentally determined in Chapter 3.1.1.

The prepared crushed raw material was weighed according to the designed clay-glass compositions and, simultaneously, introduced in the continuously operating disintegrator (7) and was repeatedly disintegrated and mixed. Dosing process can be performed both by synchronized feeding speeds and by applying a feeding rate controlling device between disintegrators (5)–(7) and (6)–(7), respectively. The specific electrical energy consumption of disintegrator (7) is E_{sp} = 4.4 kWh·t^{-1}. Therefore, the total specific electrical energy consumption of the disintegrators for crushing and mixing of clay-glass powder is E_{sp} = 6.8 kWh·t^{-1}. Finally, prepared clay-glass powders are stored in tower (8).

3.5.2. Production of CHA

Production of CHA is performed with equipment parts (8)–(15), shown in Fig. 3.14. Prepared clay-glass powder, EPS, and binding agents from towers (8), (9), and (10) feed into a periodically operating rotational cylindrical granulation machine (11) with set 3-rd critical speed, characterizing rolling and freely falling aggregates.

The duration of granulation is shorter compared with durations of dying and sintering processes. Therefore, the cylindrical granulation machine (11), drying oven (12), and sintering oven (13) are separated to provide efficient periodic operation of the cylindrical granulation machine (11). The periodically operating cylindrical granulation machine and drying and sintering ovens could be replaced with a continuously operating rotational-type cylindrical granulation machine to perform all processes simultaneously, according to the designed production volume. However, the calculation of cylinder length, angle, and rotational speed should be performed, not only for theoretical but also for industrially scaled equipment.

The clay-glass-coated EPS is inserted in the rotational cylindrical drying machine (12) with a set drying temperature of 50–75 °C. During this process, separation of an exceeded amount of clay-glass powder was performed and, subsequently, inserted in the recycling stage

of the rotational cylindrical drying machine (15) at 50–75 °C and fed into the continuously operating disintegrator (7), together with fresh clay-glass powder of the same composition.

Dried EPS granules with clay-glass coating from the rotational cylindrical drying machine (12) were inserted in the rotational cylindrical sintering machine (13), with sintering temperatures from 750 °C to 900 °C, depending on the designated application of CHA. The length and speed of the rotational cylindrical sintering machine (13) was calculated in such way to provide a heating rate of 5 °C·min^{-1}, sintering duration of 30 minutes, and final cooling of the sintered CHA to 150 °C. Formed EPS decomposition vapour (during heating from 150 °C to 250 °C) blows into the catalytical oxidation reactor (14). Gaseous oxidation products with elevated temperature were used for heating material in the rotational cylindrical drying machines (12) and (15) for drying CHA (S1) and recycled clay-glass powder (S2), respectively. Sintered CHA continues to the vibrational or cylindrical sieving machines and is sorted by size (16). Sorted CHA is stored in tower (17).

3.5.3. Production of FCA

Production of FCA was performed with equipment (8) and (18)–(29), as demonstrated in Fig. 3.14. Clay-glass powder and water with electrolyte from towers (8) and (18), respectively, feed into the reactor equipped with the propeller-type mixer (20). The produced suspension, through the channel (a), enters the continuously operating rotary-mixer disperser (22). The processed suspension, through the channel (b), enters the reactor equipped with propeller-type mixer (20) by providing recirculation flow. The recirculation flow applies the required amount of foam forming agent from tower (19) and, simultaneously, applies compressed air, from compressor (23), through flow channel (g) into flow channel (a) until the foamed clay-ceramic suspension reaches the required volume inside reactor (20). Required air volume control during the process, by sampling and determination of bubble sizes, was determined by optical microscopy. All obtained foamed suspensions were processed in the rotary-mixer disperser (22), no less than 2–3 times after the compressed air supply from compressor (23), in designed volume, was used to achieve designed bubble sizes from 50 μm to 150 μm.

Suspension produced through the flow channel (c) and excess amounts of anti-agglomeration agent from tower (24) enter the periodically operating rotational cylindrical granulation machine (25) by continuing recirculation flow through channels (a) and (b) to avoid coalescence of the foamed suspension. Nozzles with diameters from 1 mm to 3 mm are exposed to shock waves vibrations, with frequencies from 0.5 Hz to 1.0 Hz, providing removal of foamed suspension droplets from nozzles. The diameter of the nozzle, foamed suspension flow rate, air content, and vibration frequency influence the final size and porosity of the FCA. Coated FCA enters the rotational cylindrical drying machine (26) with a set drying temperature of 50–75 °C. Excessive amounts of dry anti-agglomeration powder move to tower (24) for repeated use in the periodically operating rotational cylindrical granulation machine (25).

Dried FCA inserts into the rotational cylindrical sintering machine (27), with sintering temperatures from 750 °C to 900 °C, depending on the FCA application. The duration of FCA

granulation is much shorter compared to the drying and sintering processes. Therefore, devices (25)–(27) are separated to provide efficient periodical operation of the rotational cylindrical granulation machine (25), avoiding the production of too much FCA inter-product. The length and speed of rotational cylindrical sintering machine (27) is determined to provide a heating rate of 5 °C·min^{-1}, sintering duration of 30 minutes, and final cooling of sintered FCA to 150 °C. Importantly, the periodically operating cylindrical granulation machine and drying and sintering ovens can be replaced with a continuously operating rotational-type cylindrical granulation machine to perform all processes simultaneously, according to designed production volume. However, the calculation of cylinder length, angle, and rotational speed should be performed, not only for theoretical, but also for industrially scaled equipment.

Formed flue gas, with elevated temperature from the rotational cylindrical sintering machine (27), transferred through flow channel (S7) into the rotational cylindrical drying machine (26). Sintered FCA was inserted in the vibrational or cylindrical sieving machines and sorted by sizes (28). Sorted FCA is stored in tower (29).

3.5.4. Production of CCF Blocks

Production of CCF blocks was performed with equipment parts (8), (17)–(21), and (27)–(31), shown Fig. 3.14. Clay-glass powder and water with electrolyte from towers (8) and (18), respectively, feed in the reactor equipped with the propeller-type mixer (20). The produced suspension enters the continuously operating rotary-mixer disperser (22) through channel (a). Processed suspension enters the reactor equipped with the propeller type-mixer (20) through channel (b), by providing recirculation flow. In recirculation flow, the required amount of foam forming agent is applied from tower (19) and, simultaneously, compressed air, from compressor (23), comes through flow channel (g) in flow channel (a), until the foamed clay-ceramic suspension reaches the required volume inside reactor (20). Required air volume control was achieved during the process, by sampling and bubble size determination, with the use of an optical microscope. Experimentally, all obtained foamed suspensions were processed in the rotary-mixer disperser (22), no less than 2–3 times after the compressed air supply, from compressor (23), was added in a designated volume, to achieve the desired bubble sizes (50–150 μm). Through channel (d), the produced suspension entered mould (30). Then, the filled mould entered drying chamber (31). The remaining heat from drying ovens (12) and (26) and flow channels (S4) and (S6) were used to dry the foamed suspension. Dried foamed clay blocks entered in the tunnel-type oven (32). The length and speed of the transporter provided a heating rate of 5 °C·min^{-1}, sintering duration of 30 minutes, and final cooling of sintered CCF blocks down to 150 °C. Cooled CCF blocks moved to storage (33).

The described production schemes for CHA, FCA, and CCF blocks utilize the same devices in the first stage of production. The use of one set of devices for manufacturing different products decreases expenditures. Further, the use of different anti-agglomerating agents (clay and peat powders), lead to two types of products, FCA with either dense or highly porous external surfaces.

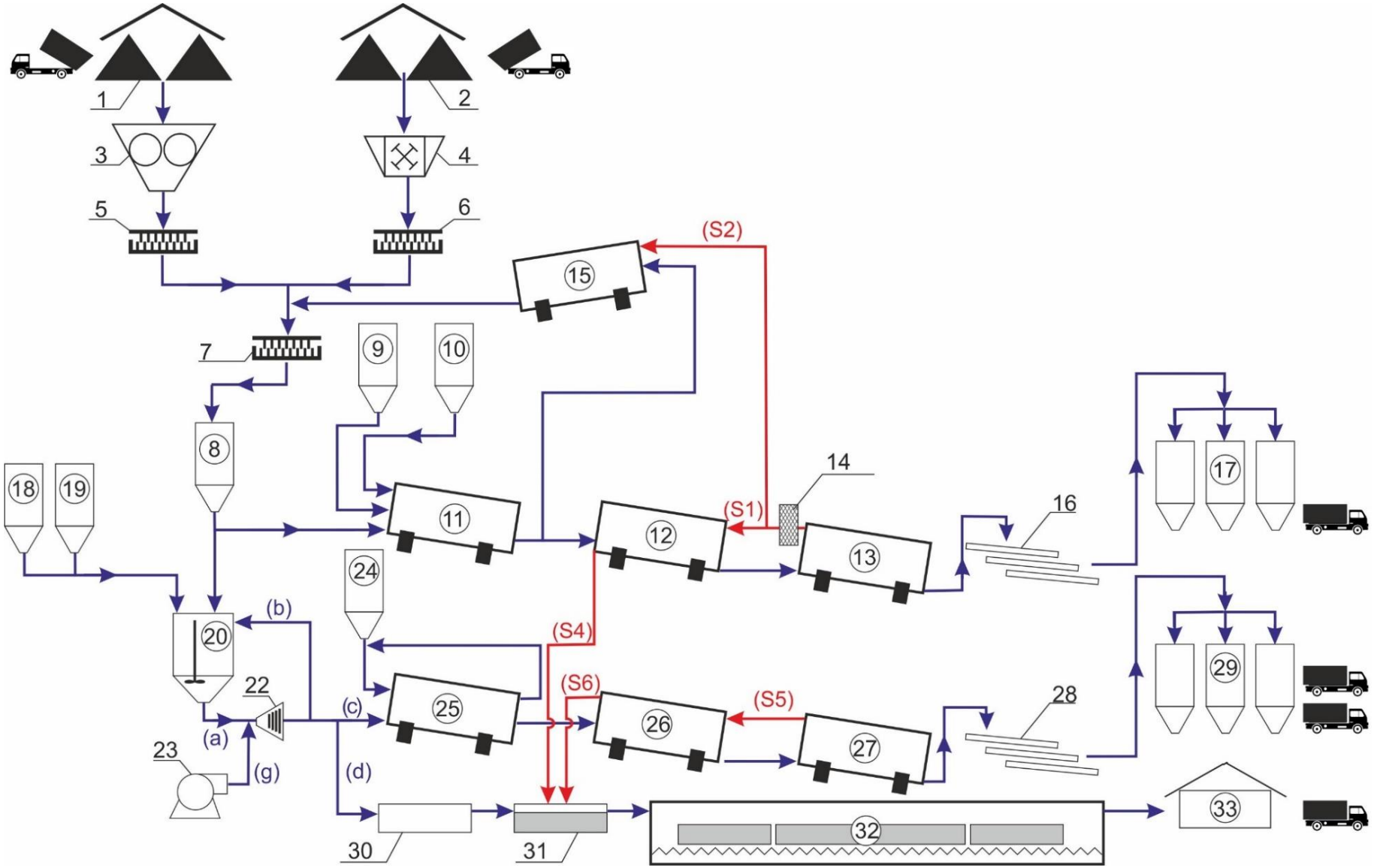

Fig. 3.14. Technological scheme for production of porous ceramic materials (CHA, FCA, and CCF blocks).

CONCLUSIONS

1. The work investigates clay-glass ceramics containing from 5 % to 15 % milled cullet (Na-silicate glass) and fired in the temperature range from 700 °C to 1050 °C. Glass additives have been found to reduce the sintering temperature of clay ceramics by an average of 60–70 degrees, with the formation of a cristobalite phase at a treatment temperature of 900 °C and the formation of a diopside starting at a treatment temperature of 800 °C.
2. The obtained clay-glass ceramics are characterized by higher compressive strength, on average twice as high at glass content >10 % and processing temperatures higher than 900 °C, compared to clay ceramics without additives. At the same time, glass additives reduce the water absorption and porosity of the obtained ceramics by 2–3 times in the whole range of studied compositions and processing temperatures, which is important in predicting the spheres of application of the material.
3. Using the studied clay-glass compositions, a method for obtaining ceramic hollow granules by the sacrificial template approach has been developed, the optimal technological parameters of granulation have been determined. The obtained granules are characterized by a well-developed surface – rounded protrusions, the average height of which is 0.8–1.5 mm. The maximum strength of the granules by pressing in the cylinder is achieved at a firing temperature of 1000 °C and a glass content of 13–15 % in the batch. The obtained granules were used for the production of experimental building blocks, which in their strength are practically twice as large as for analogous keramzite-concrete blocks.
4. The sorption properties of clay-glass ceramic foam have been studied in the dissertation, the possibility of using them as adsorbents for binding textile dyes from wastewater has been shown. Using the system ceramic foam – anionic Bezaktiv Turquise Blue V-G dye as a model of the adsorption process, the possible mechanism of the adsorption process has been studied. Using adsorption kinetic models and adsorption isotherms Langmier and Freindlich models, it was concluded that dye sorption on the ceramic sorbent surface has a complex nature, which is limited by both external and internal diffusion processes on the sorbent active centres, as well as chemical interactions between them.
5. Possibilities of practical use of foam clay ceramics containing glass additives have been researched and offered: by filling *Keraterm* clay building blocks with foamed material, it is possible to reduce their thermal conductivity coefficient up to 20 %. Using the developed granulation method, two types of granules with good petroleum product binding capacity of up to 0.95 $g \cdot g^{-1}$ in the case of FCA-P were obtained from the foamed material. The obtained granules can be used to maintain soil moisture, their water holding capacity reaches 0.26 $mL \cdot cm^{-3}$, which lags behind perlite (0.44 $mL \cdot g^{-1}$), but exceeds the water holding capacity of the widely used expanded clay (0.15 $mL \cdot g^{-1}$).
6. The present research resulted in a new technological scheme for the production of porous ceramic materials (CHA, FCA, and CCF blocks) by implementing the developed technology, manufacturing approach, and clay-glass ceramic composites.

REFERENCES

[1] V. Segliņš, "Valsts pētījumu programmas projekta 'Zemes dzīles' svarīgākie rezultāti un perspektīvas", *Mater. Sci. Appl. Chem.*, vol. 29, no. 29, p. 7, Feb. 2014.

[2] Anne Marie Mohan, 'EU glass packaging recycling rate is stable at 74% | Greener Package', 2019. [Online]. Available: https://www.greenerpackage.com/recycling/eu_glass_packaging_recycling_rate_stable_74. [Accessed: 04-Sep-2019].

[3] Eurostat, 'Municipal waste landfilled, incinerated, recycled and composted in the EU-27, 1995 to 2015', 2017. [Online]. Available: http://ec.europa.eu/eurostat/statistics-explained/index.php/File:Municipal_waste_landfilled,_incinerated,_recycled_and_composted_in_the_EU-27,_1995_to_2015_update.png. [Accessed: 19-Oct-2017].

[4] Eurostat, 'Packaging waste statistics – Statistics Explained', 2017. [Online]. Available: http://ec.europa.eu/eurostat/statistics-explained/index.php/Packaging_waste_statistics. [Accessed: 19-Oct-2017].

[5] G. Taveri, J. Tousek, E. Bernardo, N. Toniolo, A. R. Boccaccini, and I. Dlouhy, 'Proving the role of boron in the structure of fly-ash/borosilicate glass based geopolymers', *Mater. Lett.*, vol. 200, pp. 105–108, 2017.

[6] M. Marangoni, B. Nait-Ali, D. S. Smith, M. Binhussain, P. Colombo, and E. Bernardo, 'White sintered glass-ceramic tiles with improved thermal insulation properties for building applications', *J. Eur. Ceram. Soc.*, vol. 37, no. 3, pp. 1117–1125, 2017.

[7] A. Rincón, M. Marangoni, S. Cetin, and E. Bernardo, 'Recycling of inorganic waste in monolithic and cellular glass-based materials for structural and functional applications', *J. Chem. Technol. Biotechnol.*, vol. 91, no. 7, pp. 1946–1961, 2016.

[8] M. Marangoni *et al.*, 'Porous, Sintered Glass-Ceramics from Inorganic Polymers Based on Fayalite Slag', *J. Am. Ceram. Soc.*, vol. 99, no. 6, pp. 1985–1991, 2016.

[9] İ. B. Topçu and M. Canbaz, 'Properties of concrete containing waste glass', *Cement and Concrete Research*, vol. 34, no. 2. pp. 267–274, 2004.

[10] GlassAlliance, 'Statistical report 2018-2019', Brussels, 2020.

[11] M. A. Abuh, C. A. Agulanna, P. E. Chimezie, and J. U. Bethel-Wali, 'Implications and characterization of waste glass cullet – kaolinite clay ceramics', *J. Appl. Sci. Environ. Manag.*, vol. 23, no. 3, p. 513, 2019.

[12] O. M. Olofinnade, A. N. Ede, and J. M. Ndambuki, 'Experimental investigation on the effect of elevated temperature on Compressive strength of concrete containing waste glass powder', *Int. J. Eng. Technol. Innov.*, vol. 7, no. 4, pp. 280–291, 2017.

[13] M. T. Souza, B. G. O. Maia, L. B. Teixeira, K. G. de Oliveira, A. H. B. Teixeira, and A. P. Novaes de Oliveira, 'Glass foams produced from glass bottles and eggshell wastes', *Process Saf. Environ. Prot.*, vol. 111, pp. 60–64, Oct. 2017.

[14] Eiropas Komisija, 'Eiropas parlamenta un padomes direktīva 2012/27/es', *Eiropas Savienības Oficiālais Vēstnesis*, 2012. [Online]. Available: https://eur-lex.europa.eu/legal-content/LV/TXT/HTML/?uri=CELEX:32012L0027&from=LV. [Accessed: 10-Aug-2019].

[15] S. Keraterm, ‘Celtniecības bloks KERATERM 25 : Lode’. [Online]. Available: http://www.lode.lv/lv/keramiskie-bloki/keramiskais-celtniecibas-bloks-keraterm-25. [Accessed: 18-Dec-2016].
[16] P. Colombo, ‘Conventional and novel processing methods for cellular ceramics.’, *Philos. Trans. A. Math. Phys. Eng. Sci.*, vol. 364, no. 1838, pp. 109–24, Jan. 2006.
[17] C. Moreno-Castilla, ‘Adsorption of organic molecules from aqueous solutions on carbon materials’, *Carbon*, vol. 42, no. 1. pp. 83–94, 2004.
[18] S. Kushwaha, H. Soni, V. Ageetha, and P. Padmaja, ‘An Insight Into the Production, Characterization, and Mechanisms of Action of Low-Cost Adsorbents for Removal of Organics From Aqueous Solution’, *Crit. Rev. Environ. Sci. Technol.*, vol. 43, no. 5, pp. 443–549, 2013.
[19] Z. Zhang and B. Wang, ‘Preparation and properties of clay-based air-permeable and water-retention material’, *Procedia Eng.*, vol. 27, no. 2011, pp. 475–481, Jan. 2012.
[20] J. Kers, P. Kulu, D. Goljandin, and V. Mikli, ‘Reuse of reinforced acrylic plastic waste in new composite material development’, in *Proceedings of the International Conference of DAAAM Baltic ‘Industrial Engineering’*, 2006, pp. 267–272.
[21] V. R. Salvini, B. a. Sandurkov, R. F. K. Gunnewlek, D. S. Rosa, and V. C. Pandolfelli, ‘Porous ceramics with tailored properties’, *Am. Ceram. Soc. Bull.*, vol. 86, no. 3, pp. 9401–9405, 2007.
[22] A. R. Studart, U. T. Gonzenbach, E. Tervoort, and L. J. Gauckler, ‘Processing Routes to Macroporous Ceramics: A Review’, *J. Am. Ceram. Soc.*, vol. 89, no. 6, pp. 1771–1789, Jun. 2006.
[23] O. Muter *et al.*, ‘Comparative study on bacteria colonization onto ceramic beads originated from two Devonian clay deposits in Latvia’, no. March 2015, pp. 134–140, 2012.
[24] D. M. Ibrahim and M. Helmy, ‘Crystallite growth of rice husk ash silica’, *Thermochim. Acta*, vol. 45, no. 1, pp. 79–85, Apr. 1981.
[25] A. Fluegel, ‘Glass viscosity calculation based on a global statistical modelling approach’, *Glas. Technol. Eur. J. Glas. Sci. Technol. Part A*, vol. 48, no. 1, pp. 13–30, 2007.
[26] M. F. Ashby, *Materials Selection in Mechanical Design*, Fourth. Oxford: Butterworth Heinemann, 2010.
[27] W. Weber, J. Morris, and J. Sanit, ‘Kinetics of Adsorption on Carbon from Solution’, *J. Sanit. Eng. Div.*, vol. 89, pp. 31–38, 1963.
[28] A. Ozer, ‘Removal of Pb(II) ions from aqueous solutions by sulphuric acid-treated wheat bran’, *J. Hazard. Mater.*, vol. 141, no. 3, pp. 753–761, Mar. 2007.
[29] A. L. Ahmad, C. Y. Chan, S. R. Abd Shukor, and M. D. Mashitah, ‘Adsorption kinetics and thermodynamics of β-carotene on silica-based adsorbent’, *Chem. Eng. J.*, vol. 148, no. 2–3, pp. 378–384, May 2009.
[30] С. Лилия, ‘Сорбция фосфатидилхолина наноструктурированными полистиролами и кремнийсодержащими материалами’, Воронежский государственный университет инженерных технологий, 2016.

[31] S. Lagergren, ‘Zur Theorie der sogenannten Adsorption gelöster Stoffe, Kungliga Svenska Vetenskapsakademiens’, *Handlingar*, vol. 24, no. 4, pp. 1–39, 1898.

[32] Y. Ho and G. McKay, ‘A kinetic study of dye sorption by biosorbent waste product pith’, *Resour. Conserv. Recycl.*, vol. 25, no. 3–4, pp. 171–193, Mar. 1999.

[33] C. Escudero, N. Fiol, I. Villaescusa, and J. C. Bollinger, ‘Arsenic removal by a waste metal (hydr)oxide entrapped into calcium alginate beads’, *Journal of Hazardous Materials*, vol. 164, no. 2–3. pp. 533–541, 2009.

[34] H. Qiu, L. Lv, B. Pan, Q. Zhang, W. Zhang, and Q. Zhang, ‘Critical review in adsorption kinetic models’, *J. Zhejiang Univ. A*, vol. 10, no. 5, pp. 716–724, May 2009.

[35] A. Behnamfard and M. M. Salarirad, ‘Equilibrium and kinetic studies on free cyanide adsorption from aqueous solution by activated carbon’, *Journal of Hazardous Materials*, vol. 170, no. 1. pp. 127–133, 2009.

[36] M. Thommes *et al.*, ‘Physisorption of gases, with special reference to the evaluation of surface area and pore size distribution (IUPAC Technical Report)’, *Pure Appl. Chem.*, vol. 87, no. 9–10, pp. 1051–1069, Oct. 2015.

[37] Y. S. Ho and G. McKay, ‘Pseudo-second order model for sorption processes’, *Process Biochem.*, vol. 34, pp. 451–465, 1999.

[38] K. V. Kumar, ‘Pseudo-second order models for the adsorption of safranin onto activated carbon: Comparison of linear and non-linear regression methods’, *J. Hazard. Mater.*, vol. 142, no. 1–2, pp. 564–567, Apr. 2007.

[39] I. Langmuir, ‘The constitution and fundamental properties of solids and liquids. II. Liquids’, *J. Am. Chem. Soc.*, vol. 39, no. 9, pp. 1848–1906, Sep. 1917.

[40] Schlagmann_Poroton, ‘POROTON-S8’, 2013. [Online]. Available: http://www.schlagmann.de/poroton-s-acht. [Accessed: 10-Dec-2016].

[41] X. Yang, B. Yang, M. Gao, and C. Ye, ‘An internal core cast composite self-insulation foam concrete block and its preparation method’, CN 103306422 B, 2013.